

1 Genomic Evidence of Fisheries Induced Evolution

2 in Eastern Baltic cod

3 Kwi Young Han^{1*}, Reid S. Brennan¹, Christopher T. Monk¹, Sissel Jentoft², Cecilia
4 Helmerson², Jan Dierking¹, Karin Hüsse³, Érika Endo Kokubun¹, Janina Fuss⁴, Ben Krause-
5 Kyora⁴, Tonny B. Thomsen⁵, Benjamin D. Heredia⁵, Thorsten B.H. Reusch¹

6

7 ¹ GEOMAR Helmholtz Centre for Ocean Research Kiel, Kiel, Germany

8 ² Centre for Ecological and Evolutionary Synthesis (CEES), Department of Biosciences,
9 University of Oslo, Oslo, Norway

10 ³ National Institute of Aquatic Resources, Technical University of Denmark, Kgs. Lyngby,
11 Denmark

12 ⁴ Institute of Clinical Molecular Biology, Christian-Albrechts-University of Kiel, Kiel 24105,
13 Germany.

14 ⁵ Geological Survey of Denmark and Greenland, Copenhagen, Denmark

15 *Corresponding author. Email: khan@geomar.de

16

ABSTRACT

17 Humans have become one of the greatest evolutionary forces, and their
18 perturbations are expected to elicit strong evolutionary responses. Accordingly, during (size)
19 selective overharvesting of wild populations, marked phenotypic changes have been
20 documented, while the evolutionary basis is often unresolved. Time-series collections
21 combined with genomic tools present unique opportunities to study how evolutionary
22 changes are manifested at the genome-wide level. Here, we take advantage of a unique
23 temporal dataset from the overexploited Eastern Baltic cod (*Gadus morhua*) population that
24 exhibited a 48% decrease in asymptotic body length over the last 25 years. A genome-wide
25 association study revealed pronounced peaks of outliers linked to growth performance. The
26 contributing loci showed signals of directional selection with significantly high autocovariance
27 in the allele frequency and excessive intersections with regions of high F_{st} as well as genes
28 relevant to growth and reproduction. Moreover, pattern of directional selection for ancestral
29 haplotype of the well-known chromosomal inversions in Atlantic cod (on linkage group 12)
30 was observed, while the double crossover (~1Mb) harbouring the vitellogenin genes within
31 this region showed signs of drift or balancing selection. Our results demonstrate evident
32 response of the genome over a relatively short time frame and further underscore
33 implications for fisheries management and conservation policy regarding the adaptive
34 potential of marine populations.

35 INTRODUCTION

36 Human beings play a significant ecological and evolutionary role as they manipulate
37 and disrupt environments and organisms by habitat alteration, pollution, climate change and
38 harvesting (Palumbi 2001). This impact extends beyond a population's distribution and its
39 relevant ecological landscape of one time point and influences future generations by exerting
40 strong selective pressures (Vitousek et al. 1997; Palumbi 2001; Hendry, Gotanda, and
41 Svensson 2017). Rapid evolutionary changes caused by anthropogenic pressures, e.g.,
42 overfishing, pose special challenges in detecting induced selection processes, as the
43 changes usually span a relatively short time frame insufficient for a conventional sweep-like
44 pattern causing the complete fixation of focal alleles. Here, historical time-series samples
45 provide a special lens to the past in detecting evolution in action by enabling direct access to
46 allele frequency changes in genomic data (Franssen, Kofler, and Schlötterer 2017). In the
47 context of fisheries induced evolution, one of the strongest human perturbations caused by
48 size selectivity or added mortality onto a fish population, so far, the only compelling evidence
49 for genome-level responses to overfishing comes from a 40 years of annual time series data
50 of Atlantic salmon. A clear decrease in age at maturity in Atlantic salmon was accompanied
51 by directional change in the allele frequency of *vgl3* gene (Erkinaro et al. 2019; Czorlich et
52 al. 2018), a large effect locus explaining 39% of the phenotypic variation (Barson et al. 2015;
53 Ayllon et al. 2015), which was significantly correlated with fishing pressure for the target
54 species as well as a food species in salmon aquacultures (Czorlich et al. 2022). However, as
55 most traits under fishing induced selection, including life history traits like growth rate, have a
56 polygenic basis with a large number of small effect loci, challenges remain in both the
57 identification of the contributing loci and the detection of subtle changes in frequency of the
58 loci (see (Reid, Star, and Pinsky 2023; Pinsky et al. 2021)).

59 Eastern Baltic cod (EBC) is an Atlantic cod (*Gadus morhua*) population residing in
60 the central Baltic Sea, with the last remaining spawning ground being the Bornholm Basin
61 (ICES 2022). The population diverged from other Atlantic cod populations 7-8 thousand
62 years ago when the Baltic Sea with its current salinity regime emerged after a series of
63 postglacial tectonic shifts in combination with sea-level changes (Matschiner et al. 2022;
64 Schmölcke et al. 2006; Martínez-García et al. 2021). Currently, it is biologically and
65 genetically differentiated from all other ecotypes, e.g. western Baltic (WBC) and North Sea
66 cod and adapted to the peculiar Baltic environment and experiences low salinities, high
67 pCO₂, prevalent hypoxia, and inconsistent and highly variable seasonal patterns of
68 temperature, salinity and oxygen contents (Reusch et al. 2018; Zillén et al. 2008;

69 Stockmayer and Lehmann 2023). These fluctuating environmental conditions have
70 contributed to the indistinguishable pattern in the otolith rings for age readings,
71 compromising the age-related data for stock assessments of EBC (Heimbrand et al. 2020).
72 At present, EBC is isolated from neighbouring WBC in the absence of genetic inflow (Paul R.
73 Berg et al. 2015; Hemmer-Hansen et al. 2019), even though some limited hybridization
74 occurred historically, at high population abundance (Helmerson et al. 2023).

75 EBC plays a major role not only ecologically as a key predator species in the food
76 web, particularly notable in the Baltic's uniquely low biodiversity (Ojaveer et al. 2010), but
77 also economically as it has been fished recreationally and was the largest target species for
78 commercial fisheries with an annual catch of up to 400,000 tons in the mid-1980s (ICES
79 2022). However, overfishing and size-selective fishing continued with excessively high total
80 allowable catch resulting in fishing mortality typically 2-3 times higher than the maximum
81 sustainable yield (MSY) (Birgersson 2022; ICES 2019; Eero et al. 2011; Zeller et al. 2011).
82 Since the mid-1990s, multiple aspects of the EBC population have been deteriorating and
83 have recently reached the unprecedented lowest point in their state since the 1950s
84 (Birgersson 2022; Eero et al. 2023). The spawning stock biomass (fish sized over 35cm) has
85 declined sharply in recent years, together with recruitment and loss of two major spawning
86 grounds (Cardinale and Svedäng 2011; Köster et al. 2017). Higher mortality on older
87 individuals can lead to size truncation, growth retardation, and worsened condition (weight-
88 at-length) (Eero et al. 2023; Möllmann et al. 2009; Svedäng and Hornborg 2014; 2017). The
89 size at first maturity and condition of the fish marked the lowest value of L50 (length at 50%
90 of population reaches maturity) under 20 cm in recent years (Eero et al. 2015; ICES 2021;
91 Mion et al. 2021; Svedäng and Hornborg 2017). A complete collapse of the stock has
92 resulted in a ban on targeted fishing on EBC since 2019 (ban renewed for 2024) but the
93 condition of the population has not been able to recover to a healthy status so far.

94 Despite the prominent changes in body length in the EBC, the genetic basis of the
95 change, thus the evolutionary consequences of overfishing, has not been investigated until
96 now. Here, we investigated whether or not changes in a heritable trait under selection
97 caused by size-selective trawling translates to a detectable response of the genomes over
98 time. To this end, we modelled individual growth using archived otoliths and sequenced
99 whole-genomes of the population over multiple time points in the period of 1996-2019
100 (referred as "temporal population" hereafter). Individuals caught in Bornholm Basin (Figure
101 1A) were selected to cover the full breadth of time and phenotype spectrum, by random
102 sampling along the length distribution for each time point (a sample set called "random"
103 hereafter), then including individuals at the both tails of the distribution (called "phenotype").
104 A genotype-phenotype association study (GWAS) identified pronounced peaks of outlier loci
105 near genes linked to growth and maturity, which in turn showed signals of selection. In

106 parallel, we found a heterogeneous pattern of selection in a large inverted region in linkage
107 group (LG) 12. This study is, to the best of our knowledge, the first in a fully marine species
108 to provide leads that suggest genomic changes to underlie phenotypic evolution of a
109 polygenic trait in response to overfishing in the field. It showcases the strength of combining
110 temporal genomics of wild population with its phenotype data and eventually guides us
111 through connecting dots of fisheries induced evolution.

112

113 RESULTS

114 Temporal Changes in Growth Rates

115 To demonstrate a phenotypic change under size-selective fishing pressure over the
116 last 25 years (1996-2019), we focused on individual growth rates as the key heritable trait.
117 We first aged archived otolith samples of 152 EBC individuals from Bornholm Basin using a
118 novel method of biochemical reading as age information of EBC recorded through a
119 conventional method has been unreliable (Hüssy et al. 2021). The oldest fish was a 7-year-
120 old caught in 1996 while individuals as old as 5 years old could be sampled in more recent
121 years (2014 and 2019) (Table S1). Using the distance from the core to each chemical
122 annulus, the estimated otolith radii, von Bertalanffy growth parameters were estimated for
123 each fish individual and each temporal population (von Bertalanffy 1957); Table S2). Fish in
124 1996 grew to reach a larger terminal maximum size, and had a smaller Brody growth
125 coefficient k , meaning they took longer to approach their terminal length than fish from
126 recent years. The median of estimated individual length at infinity, L_∞ , decreased by 48%
127 from 1996 to 2019, with a small inconsistency in 2008 (Figure 1B and S1A). Remarkably,
128 this translates to a maximal fish length (L_∞) decrease from 1150 mm in 1996 to 539 mm in
129 2019 when back-calculating fish body length from otolith radii. Accordingly, growth
130 coefficient k increases over the period with the same trend in 2008 in both group parameters
131 and individual parameters (Figure S1B). A growth performance index (Φ) for each fish of
132 different years, which summarises the growth (Moreau, Bambino, and Pauly 1986), showed
133 a consistent decrease in time (Figure 1C). Additionally, the otolith radii at age 1 for all fish
134 were back-calculated to body length and compared to examine any deviation in the juvenile
135 growth of EBC in temporal trend (Figure S1C). Although mean distances to the first-year
136 radii do not differ, the variance of the radii significantly reduced over time (Bartlett's test for
137 variance, p -value = 0.02868), indicating truncated phenotypic diversity in juvenile growth.
138 Here, the condition of individual fish at catch (relative condition factor (Le Cren 1951))
139 showed statistically different population mean only for 2002 (Figure S2A). When tested for

140 correlation, individuals' condition did not predict either the growth parameters, L_∞ and k , or Φ
141 ($r = -0.03$ ($p > 0.05$)), $r = 0.09$ ($p > 0.05$), and $r = 0.09$ ($p > 0.05$) respectively). (Figure S2B-
142 D). Overall, this supports that the population has shifted to grow slower and reach smaller
143 size when older during the study period of heavy fishing pressure.

144

145 **Genome-wide Temporal differentiation**

146 In order to investigate any temporal differentiation of EBC which might potentially
147 correspond to the phenotypic change, we subjected a set of 5,847,389 SNPs (MAF > 0.005)
148 identified for 115 "random" samples to population summary statistics. First, a principal
149 component analysis (PCA) using SNPs outside previously reported large chromosomal
150 inversions revealed a panmictic population structure among time points (Figure 1D). The
151 variances explained by PC1 and PC2 were relatively small (1.26 and 1.03%) while the
152 loadings for each PC were well distributed along the whole genome. Second, we applied a
153 temporal covariance analysis developed by Buffalo and Coop (Buffalo and Coop 2019;
154 2020) to test genome-wide pattern of selection signature. The pairwise autocovariance of
155 allele frequency changes in all time windows showed a pattern that resembled that of a
156 simulated neutral scenario (Figure S3 and S4). The observed temporal autocovariance
157 values from the samples were within the distribution of the expected under drift ($p > 0.05$ for
158 all paired autocovariances), which shows a lack of genome-wide selection signal (Figure
159 S5). Lastly, genome-wide nucleotide diversity (π) and absolute divergence between
160 populations (d_{xy}), calculated for 50 kb - windows varied only little among years (Figure S6).
161 As expected, windowed π and d_{xy} varied along linkage groups depending on differences in
162 recombination rate along the chromosome, e.g. centromere regions featuring less
163 recombination (Sardell and Kirkpatrick 2020; Tigano et al. 2021). Some divergence was
164 observed at the beginning of LG2 and in the central section of LG7, which were most likely
165 caused by the varying frequency of the inverted regions. Overall pattern shows comparable
166 genome-wide π (ranging from lowest value of 0.0071 for 1996 to highest value of 0.0077 for
167 2008) and consistent slight increase in d_{xy} values as the sampling points are more distant,
168 which indicates drift over time.

169

170 **Genotype-Phenotype Association and Selection of SNPs linked to growth**

171 In the lack of genome-wide signal of selection, we sought to identify loci under
172 directional selection by a genome-wide association (GWA) analysis using individual growth
173 performance index (Φ) as a phenotype and 679,584 biallelic SNPs (MAF > 0.05). Three
174 regions of the genome were clear outlier peaks with $-\log_{10}P$ values around 6 and most likely
175 to be associated with growth performance (Figure 2). The distribution of moderate p-values
176 ($3 < -\log_{10}P < 5$) across the genome in itself shows the polygenic nature of growth as well as

177 the methodological limitations of GWA analysis given our relatively low sample size of 152.
178 Under a formal correction for multiple testing only a few regions remained at $p = 0.05$. As
179 this study was designed as an explorative approach, an outlier status was assigned to 338
180 SNP loci that lie in the lowest 0.05% of the distribution of p-values.

181 Regions with a peak of clustered outliers with flanking SNPs with low p-values were
182 examined in depth to seek biological relevance of the SNP sites. Genes which span over 5
183 Kb up- and downstream of the outliers were listed as candidate genes linked to growth
184 variations. Amongst these candidate genes, the three most evident peaks of outliers in LG3,
185 LG6 and LG14 contained genes which were most relevant to growth or maturity from
186 functional annotation and previous research (Figure 2B-D, Table 1): LG3 contains *ncapg*,
187 which is differentially expressed in puberty in salmon (Crespo et al. 2019) and *fam184b*,
188 which is associated with body weight at first egg in chicken (Fan et al. 2017). Linkage group
189 6 included *pde4d* gene which showed response in the transcriptome of fast growth line in a
190 rainbow trout (Cleveland, Gao, and Leeds 2020). Finally, in linkage group 14 *mettl21e* which
191 was linked to growth in pupfishes and intramuscular fat deposition in cattle (Fonseca et al.
192 2020; Patton et al. 2022).

193 In order to understand if the genomic regions explaining phenotypic variation were
194 under selection through time, we calculated covariance values for the GWA outliers to
195 observe directional change in their allele frequency. Specifically, lag-2 (i.e. $\text{cov}(\Delta 1996-2008,$
196 $\Delta 2002-2014)$ and $\text{cov}(\Delta 2002-2014, \Delta 2008-2019)$) and lag-3 (i.e. $\text{cov}(\Delta 1996-2014, \Delta 2002-$
197 2019)) autocovariance (as illustrated in inlets of Figure S7) were calculated. Temporal
198 covariances of allele frequency changes of 338 outlier SNPs exhibited remarkably high
199 values of 0.00154 and 0.00187 for lag-2 and 0.00537 for lag-3 (Figure S7). Based on 1000
200 random permutations of covariance values of 338 SNPs sites, the observed covariances of
201 GWA outliers markedly exceed the ranges of null-distributions ($p < 0.001$). This result
202 strongly supports that the GWA outliers, highly correlated to the growth performance
203 collectively, experienced selection and responded accordingly with a directional frequency
204 change over time.

205

206 **Integration of the selection scan and GWAS**

207 As a complementary approach to detect directional selection of loci linked to growth,
208 we combined the GWA results with a selection test. An F_{st} scan on 20 Kb sliding windows
209 across the genome was conducted comparing the temporal population of 1996 and 2019.
210 Despite the lack of genome-wide signal of selection among temporal populations, we were
211 able to identify regions of higher differentiation (Figure 3). While the genome-wide F_{st} value
212 was xxx, a low value as expected for a single spatial population, some regions showed
213 higher F_{st} values up to 0.1. When outlier windows of 5% highest p-values were assigned to

214 intersect with GWAS outliers, 33 windows overlapped. To test the statistical significance of
215 this overlap, a null distribution was produced with a randomization test which the observed
216 values can be compared to. Based on 5000 random permutations, wherein 338 SNPs were
217 randomly chosen to overlap with the outlier windows, the observed number exceeded the
218 upper tail of the expected distribution (Figure S8). This signifies that loci associated with
219 growth performance are predicted to reside in the regions of highest F_{st} between 1996 and
220 2019. Those two lines of evidence, the positive temporal covariance values of GWA outliers
221 and their significant overlap with high F_{st} windows, strongly indicate the impact of directional
222 selection on the genetic factors under growth variations in EBC.

223 The biological significance of these overlapping regions was further explored through
224 a gene ontology (GO) term enrichment test on overlapping F_{st} windows (Table 2). Multiple
225 pathways involved in ultradian rhythm, water homeostasis, and protein metabolism, and
226 meiotic cell cycle were enriched. Ultradian rhythm is important in diverse functions including
227 growth, reproduction, and metabolism in fish (Cowan, Azpeleta, and López-Olmeda 2017;
228 Frøland Steindal and Whitmore 2019; Sánchez-Vázquez et al. 2019; Zhdanova and Reebs
229 2006). Diverse metabolic processes involving amino acids were also significantly enriched,
230 which is critical for fish growth rates (Finn and Fyhn 2010; Pelletier et al. 1994). Interestingly,
231 folic acid deficiency in diet has direct implications in fish growth (Hardy and Kaushik 2021;
232 John and Mahajan 1979; Lin, Lin, and Shiao 2011; Miao et al. 2013). The dietary
233 requirement of folic acid in fish emphasises its role in not only growth performance but also
234 diverse functions such as immune responses (Badran and Ali 2021; Trichet 2010). Pathways
235 involved in mitotic cell cycle and development (e.g., regulation of mitotic cell cycle,
236 embryonic, myotome development) together with multicellular organismal water
237 homeostasis, form a large part of the list. These pathways have in common that they relate
238 to a biological process called “oocyte maturation”. In fish, oocyte maturation takes place
239 before ovulation and is necessary for a successful fertilisation (Nagahama and Yamashita
240 2008), which may be indirectly linked to growth.

241

242 **Regions of Temporal Selection**

243 Along with selection signals observed in regions associated with growth phenotype,
244 we were able to identify selection signatures in other parts of the genome. In the F_{st} selection
245 scan, pronounced high F_{st} values in LG2 and LG12 as well as low values in LG7, where
246 previously reported inversions reside (marked in pink), were observed along with highly
247 conspicuous deviations of π values (Figure S6). Thus, we calculated the frequency of a
248 haplotype for each inversion in the temporal populations. Interestingly, only the inversion in
249 LG12 was decreasing in its frequency consistently over time (Mann-Kendall test for
250 monotonic trend: p-value = 0.03) (Figure 4). Within this inversion, another block of inverted

251 region, so called “double crossover” (DC), was reported to be private to the EBC population
252 (Matschiner et al. 2022). Thus, we identified the DC within the inversion in our sequence
253 data (Figure S9) to examine the temporal trend of its frequency. Unlike the consistent
254 decrease in the haplotype frequency of LG12, frequency of the DC within only decreases
255 until 2014 then picks up in 2019. So, it seems that while the large inversion in LG12 behaves
256 under directional selection as a whole, the DC escapes from this selection and is rather
257 either drifting or under balancing selection on its own.

258 Additionally, the highest F_{st} values outside inverted regions were spread across the
259 genome, some of which appear in peaks of clustered outliers. GO term enrichment analysis
260 was conducted using 575 genes residing within the outlier windows of top 5% (Table S3).
261 Several GO terms were enriched in sub-categories, which are highly related to the growth of
262 a fish. For example, metabolisms and processing of macromolecules such as amino acids,
263 fatty acids, and carbohydrates which in turn are key to any growth process. Fatty acid
264 oxidation is strongly related to use of energy sources in response to feeding conditions (J. Ø.
265 Hansen et al. 2008; Stubhaug, Lie, and Torstensen 2007; Turchini and Francis 2009) and
266 cAMP biosynthesis is part of processing ATP, which is also critical in regulations of
267 hormones involved in metabolism and reproductions (Miki, Van Heerden, and Fitzpatrick
268 1997; Takahashi and Ogiwara 2023). Also, regulation of TOR pathway, which is crucial in
269 sensing growth hormone, nutrient or oxygen condition (Dobrenel et al. 2016; Hietakangas
270 and Cohen 2009), was found to be enriched. As expected, some enriched biological
271 pathways do not always show direct relevance to growth. Other highly represented clusters
272 of GO term are in regard to developments such as gastrulation, convergent extension
273 involved in axis elongation, and tissue morphogenesis. Interestingly, regulation of neural
274 retina development together with melanosome transport, which is involved retinal
275 pigmentation, may suggest temporal differentiation in the visual sensory system in EBC
276 which is potentially relevant to depth adaptation, thus vertical movements (P. R. Berg et al.
277 2017; Pampoulie et al. 2015).

278

279 DISCUSSION

280 This study identifies, for the first time to our knowledge in an exploited marine fish
281 population, the genomic regions with associated gene functions that are linked to growth
282 impairment. Reassuringly, they were also found to be under directional selection using
283 genome scans and temporal covariance approaches. Temporal selection was likely driven
284 by strong and documented overfishing on Eastern Baltic cod that ultimately led to the life-

285 history change by fisheries induced evolution. A drastic decrease in the individual growth is
286 accompanied by the contributing loci demonstrating clear evidence of directional selection
287 with significantly positive temporal autocovariances of allele frequency changes and an
288 excess number of overlaps with regions of high F_{st} . The combination of a selection test and
289 GWA used here is a powerful implementation of detecting an adaptive polygenic trait (Bosse
290 et al. 2017; Brennan et al. 2018; Barghi, Hermissen, and Schlötterer 2020), which have
291 responded to a selective pressure. In addition, observed directional change in the frequency
292 of ancestral haplotype of inversion in LG12 but not for its double crossover region
293 underscores the heterogeneous response of the genome under selection.

294

295 **Overall Patterns of Temporal Genomic Change**

296 Non-significant change of nucleotide diversity, a lack of clustering pattern in PCA,
297 and genome-wide covariance patterns resembling neutral population suggest that migration,
298 gene flow and other non-adaptive processes were negligible over the study period, at least
299 not at the resolution provided by the methods employed. In addition, heterogeneous
300 response of the genome, by utilising standing genetic variation across the genome, may
301 have been driving the changes in phenotype potentially through different metabolic
302 processes (Crespel et al. 2021). Hence, the premise of this study, namely that EBC is a
303 closed, self-sustained gene pool without immigration of divergent genotypes, is supported.
304 Moreover, the possibility of other traits undergoing selection or drift in divergent directions
305 than the targeted trait, could potentially obscure the genome-wide signal of size selective
306 fishing in wild populations. For example, in EBC, an opposing selection pressure against
307 small female body size can be hypothesised. This is because larger females produce larger
308 and more buoyant eggs that permit them to float higher in the water column (Nissling and
309 Vallin 1996), away from the near-bottom where the oxygen conditions are worsening.

310 Absence of evidence of overall pattern does not equate to evidence of absence of
311 selection (Bosse et al. 2017; Fuller et al. 2020). Despite the lack of overall pattern, evident
312 non-random signals were observed when targeting specific regions, the inverted region of
313 LG12 and the candidate loci of GWA. Against the background of no overall change in
314 genomic patterns (Figure S5 and S6) the directional change in the frequency of inversion in
315 LG12 clearly suggests selection in parallel to the apparent decline of growth rates. In EBC,
316 apart from some adaptive loci linked to salinity and oxygen found within the chromosomal
317 inversion in LG2 (Paul R. Berg et al. 2015), any evidence on adaptive or ecological roles of
318 inversion haplotypes is generally lacking. Although no GO term was found significantly
319 enriched for genes located within the inverted region of LG12, the ancestral homozygous
320 status of individuals, together with body size, had a correlation to lower survival rate in an
321 Atlantic cod population in the North Sea (Barth et al. 2019). In addition, SNP loci within this

322 inverted region were highly correlated with temperature and oxygen level at the surface likely
323 driving the differentiation of cod populations (Paul R. Berg et al. 2015). Interestingly, the
324 frequency of double crossover (DC) within the inverted region seems to be fluctuating
325 independently of the large inversion. This region is densely packed with genes including
326 three vitellogenin genes, which are crucial for creating buoyancy of eggs for the survival and
327 successful spawning in EBC (Nissling and Westin 1991). In this context, we speculate that
328 the selection pressure acts upon the inversion as a whole, but is relaxed for the crucial set of
329 genes in the DC by broken linkage disequilibrium. This scenario might also explain the
330 hypothesis of the opposite selection pressure on body size of females mentioned above.

331

332 **Functional relevance of selected loci**

333 Several enriched GO pathways for the overlapping regions of GWA and F_{st} outliers
334 suggest that the selected gene functions are causally linked to altered growth in EBC (Table
335 1). Light manipulation to tweak the ultradian rhythm of individuals, thus the long term
336 seasonality, is a very common method to control growth and maturity in fish aquaculture
337 including Atlantic cod (Skulstad et al. 2013; Taranger et al. 2010; Karlsen et al. 2006; T.
338 Hansen et al. 2001). Depending on the applied photoperiod, sexual maturation can be
339 controlled, either postponed or advanced, which is tightly entangled to somatic growth of a
340 fish (T. Hansen et al. 2001; Davie, Porter, and Bromage 2003). In addition, water
341 homeostasis is important in egg hydration during the oocyte maturation process to make
342 floaty eggs, which is one of the major evolutionary acquisitions for pelagic teleost fish (Fyhn
343 et al. 1999). Oocyte maturation takes place before ovulation and is necessary for a
344 successful fertilisation (Nagahama and Yamashita 2008). Specific hypotheses directly
345 connecting oocyte maturation and growth are currently lacking in the field. Nevertheless, it is
346 well conceivable that the timing of spawning, through control of oocyte maturation, may be
347 critical for successful reproduction, as maturation process is highly affected by energy
348 allocation (Roff 1993), thus tightly linked to somatic growth in a fish's lifespan. Lastly, the
349 biological process of "response to heat" is indeed highly linked to growth traits in fish.
350 Warmer temperatures as the Baltic sea has been experiencing (Meier et al. 2022), critically
351 impact the species throughout the lifespan from larva to adult stage (Oomen et al. 2022;
352 Righton et al. 2010) and are dynamically interlinked with other environmental factors such as
353 oxygen. Thus, it may suggest that the slow growth trait was also mediated or accompanied
354 by shifts in temperature response over time.

355 In spite of the obvious, functionally aligned links to growth from candidate loci, there
356 seems to be a general lack of congruency in the genetic contents compared to previous
357 studies which experimentally addressed the genomic effects of size-selective harvest
358 selection. Therkildsen et al. (2019) resequenced samples from the seminal study of Conover

359 and Munch (2002) that subjected Atlantic silversides to 5 generations of upwards and
360 downward selection with respect to body size. They listed enriched GO terms from highly
361 differentiated loci accompanied by body size changes under different harvest regimes. Data
362 from the present study found no intersection to above results, which is perhaps not
363 surprising given that Therkildsen et al. (2019) itself observed highly divergent genomic
364 responses across replicates under the same treatment. In another experimental study in
365 zebrafish, Uusi-Heikkila (2015) identified another set of genes selected by fishing pressure
366 that were also not present among the genes listed as outliers in this study. Lastly, the *vgl3*
367 and *six6* genes that are of high effective size in age at maturity in salmonids species (Barson
368 et al. 2015; Ayllon et al. 2015), a tightly linked yet different life history trait, were not found to
369 be significant in any of the present analyses. This lack of consistent patterns of identified
370 genes and pathways in this study compared to previous studies of FIE as well as among the
371 studies indicate that there are heterogeneous responses in the genome level either under
372 same phenotype changes, growth, or under same selective pressure, size-selective fishing.

373

374 **Future directions and Implications in Fisheries Management**

375 With promising results showcasing EBC as an evolving population with stunted
376 growth, this study directs to important future research agendas and implications in managing
377 the stock. First, it is important to note that these evolutionary responses occurred in the
378 context of dynamic interplays of fisheries and adverse environmental factors. Examples
379 abound that overexploitation will cause evolutionary change, but these responses are always
380 highly context dependent. Depending on the life history traits under selection and their
381 genomic architecture, strength, length, and types of selection pressure together with natural
382 selection by various environmental factors may be reinforcing or counteracting the trait
383 evolution in a convoluting manner. Environmental factors, such as hypoxia and temperature
384 increase as well as ecological variables, such as prey and predator interactions and inter-
385 species competition in the Baltic Sea, have been directly and indirectly influencing the
386 population at the same time (Casini et al. 2016; Eero et al. 2012; Limburg and Casini 2018;
387 2019; Neuenfeldt et al. 2020), which may or may not have exerted an evolutionary pressure.
388 For example, sea surface temperature has risen around 1.5 °C during the study period
389 (Siegel and Gerth, 2018) and can only maximally explain a 6 % decrease in body size
390 according to gill-oxygen limitation theory (Pauly and Cheung 2018). Then the hypoxia in the
391 bottom water in the Baltic Sea has been continuously deteriorating since the 1930s and the
392 extent to which Bornholm Basin has been directly impacted were variable depending on
393 inflow from North Sea and surrounding rivers (Carstensen et al. 2014; Stockmayer and
394 Lehmann 2023). Thus, given time-series data of an adequate resolution, direct associations

395 of genotypes and fishing pressure as well as environmental variables are an essential further
396 step to take.

397 Secondly, this study focuses on the critical period of a steep decline and lowest point
398 in growth from 1996 to 2019 and provides a contemporary snapshot of the long-term
399 population dynamics of EBC. However, it is crucial to acknowledge that growth has
400 fluctuated, with an increase during the 1960s to 1980s, followed by a noticeable decline from
401 the 1990s to the present (Mion et al. 2021). Thus, the direct causes and evolutionary
402 responses shaping the growth trend warrant further investigation within a longer timeframe,
403 preceding and succeeding the study period. Especially, when an inherent lag in evolutionary
404 response, referred to as “Darwinian debt” (Ulf Dieckman in an interview by Cookson,
405 *Financial Times*) may be contributing to the delay of recovery by compromising growth
406 potentials and population resilience (Anderson et al. 2008; Ahti, Kuparinen, and Uusi-
407 Heikkilä 2020), it urges a comprehensive examination of long-term ecological and
408 evolutionary consequences.

409 Lastly, successful management plans for EBC must incorporate evolutionary aspects
410 into their framework, e.g. introducing F_{evol} (Hutchings 2009), integrating evolutionary
411 processes into economic assessments of management plans (Eikeset et al. 2013; Schenk,
412 Zimmermann, and Quaas 2023). Having said that, the impact of such measures on fisheries
413 management may be limited at this stage as the damage has already been done. At present,
414 the evolutionary debt has been accumulated and despite the current moratorium, the stock
415 recovery falls short of expectations due to concurrent contribution of ecological and
416 environmental factors to stock condition (Eero et al. 2023). Whether this lack of recovery is
417 already one consequence of the Darwinian debt is an interesting hypothesis to explore in the
418 future.

419

420 MATERIALS AND METHODS

421 Sample Collections

422 In total 152 cod individuals were used in this study after excluding individuals which
423 were identified as either a western Baltic cod from genetic analysis (9 samples), an outlier
424 from growth analysis with measurement errors (1 samples), and of low sequencing quality (2
425 samples). Sampling was done in two different ways to cover the available time period and
426 the full range of phenotype in the sampling pool. 1) A set of samples, called “random”
427 hereafter, were randomly sampled along the length distribution for five catch years; 31 from
428 1996, 22 from 2002, 24 from 2008, 20 from 2014, and 20 from 2019. 2) As another set of

429 samples, called “phenotype” hereafter, 19 smallest mature fish and 18 largest immature fish
430 were selected from the catch year 1996-1998. As any age information of the archived
431 samples was not available, neither sample based on the cohort nor on length at first maturity
432 was possible. The rationale was that by sampling immature fish, which would be first mature
433 in the following year if they had not been caught, and small, presumably young, mature fish,
434 we attempted to cover as wide a range of phenotype variation as possible.

435 Otoliths and finclips were collected in the Baltic Sea Integrative Long-Term Data
436 Series of the research division Marine Evolutionary Ecology at GEOMAR, carried out
437 annually since 1996. They were taken on board from cod caught in Bornholm Basin (Figure
438 1A), of which their phenotype data (e.g., body length, weight, maturity stage, and sex) was
439 recorded (Table S1). Otoliths were stored in paper bags. Finclips were stored in 100%
440 ethanol at -20 °C.

441

442 **Age Reading of Otoliths**

443 As the conventional otolith reading method has not been reliable for EBC, a newly
444 developed method was employed to acquire age information of the sequenced samples in
445 order to model growth based on Hüssy et al. 2021. For chemical analysis, otoliths were
446 embedded in Epoxy resin (Struers®) and cut to have exposed surface of the core and the
447 rostral part. Trace element analysis were conducted by Laser Ablation Inductively Coupled
448 Plasma Mass Spectrometry (LA-ICP-MS) to measure magnesium (^{25}Mg), phosphorus (^{31}P),
449 and calcium (^{43}Ca), which exhibit seasonal variations in EBC (Heimbrand et al. 2020; Hüssy
450 et al. 2021). Since the elements were read from the core of an otolith to the edge, the
451 measured element traces represent the chemical characteristics of an individual’s lifespan
452 from the hatch to catch. With the measured element profile, a statistical analysis was carried
453 out to determine the age. Chemical minima were identified using local polynomial regression
454 function “loess” and “peaks” in R (R Development Core Team, 2022). The arguments were
455 set based on the settings used in age reading of tag-and-recapture cod samples in previous
456 studies. The numbers of minima in Mg and P, which suggest the fish’s exposure to the
457 coldest temperature of a year (February and March), are counted as the age of an individual
458 (Figure 2 in Hüssy et al. 2021). When the two values disagreed, the element profiles were
459 visually examined. This approach is not as stable for the signals near the otolith edge. Thus,
460 visual assessment was conducted for the samples caught in the first quarter of a year. As a
461 result, annual chemical radii for each individual, total otolith radius, as well as the age at
462 catch were extracted. The exact details of preparation of otoliths, procedures concerning LA-
463 ICP-MS, and the statistical analysis can be found in Hüssy et al. 2021.

464

465 **Modelling Individual Growth Rates**

466 To acquire a heritable phenotype that may have been affected by fishing pressure,
467 we modelled individual growth using the age information. Although it was recently confirmed
468 that the growth of EBC has impaired over last decades (Mion et al. 2021), it is crucial to
469 obtain the growth pattern of sequenced individuals to integrate genotypes and phenotype.

470 To fully utilise the hierarchical nature of the estimated otolith chemical annuli at age
471 of fish individuals from different catch years, Bayesian hierarchical modelling was applied
472 using R2jags v0.7.1 R package (Su and Yajima 2021). The von Bertalanffy growth function
473 (von Bertalanffy 1957) was fitted to distance from core to chemical annuli at age on otoliths:

474
$$L_a = L_\infty (1 - e^{-k(t_a - t_0)}),$$

475 where L_a is distance from otolith core to each chemical annulus, t_a is the estimated
476 age at the annulus, L_∞ is asymptotic length in an otolith scale, which is hypothetical otolith
477 length at age of infinity, k is a growth coefficient, and t_0 is hypothetical age when length
478 equals zero. Three levels of hierarchy included measurements of annuli at age, nested in a
479 fish individual, again nested in a group of a catch year. As a result, L_∞ and k parameters
480 were estimated for each individual and also each catch year. We took the most conservative
481 approach of priors, applying a gamma distribution for catch years and normal distribution for
482 individuals with relaxed standard deviations (details in the script). To fit the model, 100,000
483 iterations were observed for three MCMC chains and the first 10,000 were discarded as
484 burn-in. The median of Rhat values were 1.0036 and model convergence of the chains were
485 visually examined in addition (Figure S10). As an additional assessment of the model,
486 residuals were calculated from estimated otolith length from the model and observed length
487 of otolith annuli (Figure S11). Here, the variance of residuals is larger for the first year which
488 could be caused by the uneven number of observations that were fed to the model for each
489 age. Nevertheless, the overall residuals remain near zero for all years. To avoid any bias of
490 condition towards bigger fish, relative condition factor (Le Cren 1951) was used to test
491 whether fish condition could predict any of the growth parameters and Φ . Back-calculation of
492 fish length was conducted using an equation from (Hüssy, Eero, and Radtke 2018), using
493 biological intercepts specific (Campana 1990) for Baltic cod. Accordingly, L_0 , which is the fish
494 length at age 0, was set to 4.3 and O_0 , the otolith length at age 0 was set to 0.01.

495

496 **DNA Extractions**

497 For genetic materials, DNA was extracted using otoliths from earlier years (1996-
498 1998, 2002, and 2008) and fin clips from recent years, 2014 and 2019. Otoliths and finclips
499 were always handled with tools (e.g., forceps) which were cleaned with ethanol 70% and
500 sterilised in between each individual sample to avoid cross contamination. The extraction

501 procedure for both otoliths and finclips were conducted following the standard protocols from
502 either DNeasy® Blood & Tissue Kit (Qiagen, Aarhus, Denmark) or NucleoSpin® Tissue Kit
503 (Macherey-Nagel, Düren, Germany). Otoliths were fully submerged in the lysis buffer to
504 lysate any remnant tissues then removed from the buffer. The lysate then was treated as in
505 the manuals provided by the kits. Fin clips were cut into small pieces (up to 25mg),
506 submerged in a lysis buffer, then continued following the protocols. The extracted DNA was
507 purified using Qiagen QIAquick® PCR Purification Kit (Qiagen, Aarhus, Denmark). DNA
508 quality was checked with standard electrophoresis in 1% agarose gel and the quantity was
509 measured using NanoDrop™ and Qubit Assay (Thermo Fisher Scientific™, Carlsbad, USA).

510 To validate cross contamination that might have occurred during the sample
511 collection, archiving process, and DNA extraction, microsatellite (MSAT) analysis was done
512 for DNA extracted from otolith samples. Four MSAT sites were used. A multiplex PCR was
513 conducted with four primer pairs on a 96-well plate. The PCR product was mixed with Hi-Di™
514 mix (Thermo Fisher Applied Biosystems™, Carlsbad, USA) with GeneScan™ LIZ dye Size
515 standard™ (Thermo Fisher Applied Biosystems™, Carlsbad, USA). Capillary electrophoresis
516 was done with the reaction mix using ABI PRISM 3100 Genetic Analyzer (Thermo Fisher
517 Applied Biosystems™, Carlsbad, USA). The MSAT peaks were analysed using
518 GeneMarker® software (Softgenetics, State College, USA). As the chosen MSAT loci
519 typically show more than ten alleles per site in a population, when samples are mixed the
520 likelihoods of encompassing the same allele at a single MSAT locus are small and are
521 virtually zero if several such loci are combined. Thus, samples showing multiple peaks for
522 any MSAT locus were identified as cross contaminated and subsequently excluded from the
523 data set (see examples in Figure S12).

524

525 **Library Preparation and Sequencing**

526 2x100 bp paired end library preparation for 16 samples from 1996 was done in the
527 Ancient DNA Laboratory at the Institute of Clinical Molecular Biology (IKMB) as a pilot to
528 check if they should be treated specially like historic DNA samples. The details of the
529 manual library preparation can be found in the method section in Krause-Kyora et al. 2018.
530 For the finclip samples from 2014 and 2019, 2x150bp paired end libraries were prepared
531 using Illumina DNA Prep kit (Illumina, San Diego, USA) by the Competence Centre for
532 Genomic Analysis (CCGA) Kiel. These libraries (16 otolith samples from 1996 from pilot and
533 40 finclip samples from 2014 and 2019) were sequenced on Illumina 6000 S4 Flowcell
534 (Illumina, San Diego, USA) by CCGA Kiel. In the end it was concluded that older otolith
535 samples can be treated the same as the rest, yielding sequence data of comparable quality.
536 Thus, rest of the samples, including “phenotype” samples from 1996-1998 and “random”
537 samples of 1996, 2002 and 2008, were sent to Norwegian sequencing center (NSC) for

538 2x150 bp library preparation using Illumina Nextera DNA library preparation kit (Illumina, San
539 Diego, USA) followed by sequencing on Illumina NovaSeq S4 Flowcell (Illumina, San Diego,
540 USA).

541

542 **Read Processing and Variant Calling**

543 All sequenced reads from this study were processed together with published
544 population data from Barth et al. 2019, to include 23 EBC (named BOR), 22 WBC (KIE), and
545 24 North Sea (NOR) cod samples, which were later partitioned out. This was to identify WBC
546 in our samples and test for any sequencing bias in our samples (Figure S13) as well as to
547 conduct ancestry painting, which includes WBC and EBC individuals of known inversion
548 status as reference (explained below). All sequenced reads were processed following the
549 GATK best Practices workflow by Broad Institute (GATK v4.1.9.0) (Van Der Auwera et al.
550 2013). All the detailed commands, parameters, and filtering options in the bioinformatics
551 workflow are included in the provided git repository. Mapping to the reference genome of
552 Atlantic cod, gadMor3.0 (NCBI accession ID: GCF_902167405.1), the median coverage of
553 each individual ranged from 4x to 31x with a median of 12x for all samples. Two samples
554 from 1996 were excluded based on their low mapping coverage below 4x.

555 After variant calling, raw SNP variants were first hard filtered based on different
556 qualities of variant sites according to best practices. Then, only biallelic SNPs were selected
557 and filtered again based on genotyping quality, missingness, read depths, and minor allele
558 frequency (MAF) of 0.005 to produce the final variant call file in a vcf format containing
559 5,847,389 variants. When possible, this full set of variants based on MAF > 0.005 were
560 used, although some analyses were carried out using 4,685,343 variants filtered with
561 MAF>0.01 due to the processing time and resource limitation.

562 Further analyses were done with two separate sets of variants resulting from different
563 partitioning of the total sample set (also partitioned from WBC and North Sea samples), as
564 parts of the sampling was intentionally biased for “phenotype” samples as explained earlier.
565 i) 115 of “random” samples were used for the analysis identifying signatures of selection
566 over time. ii) A total of 152 samples including “random” and “phenotype” samples were used
567 for genotype-phenotype association. The subset of the master vcf file was created using
568 bcftools v1.2 (Danecek et al. 2021) then fixed sites were removed using GATK
569 SelectVariants (v4.1.9.0).

570

571 **Population Statistics and Principal Component Analysis**

572 To examine any temporal differentiation in EBC independent of phenotypic data, 115
573 “random” samples were used to compute Nucleotide diversity (π), between population
574 nucleotide divergence (d_{xy}), F_{st} and principal component analysis (PCA). For calculating π

575 and d_{xy} , guides provided by Pixy (1.2.7.beta1) (Korunes and Samuk 2021) were followed. A
576 vcf file containing invariant sites was created, using GATK GenotypeGVCFs with option –all-
577 sites followed by site filtering steps using GATK VariantFiltration with same criteria as in hard
578 filtering of variants and followed by vcftools v0.1.16 (Danecek et al. 2011) on missingness of
579 0.8 and mean read depths of 10. This filtered all-site file was combined with the final variant
580 file to create the input vcf file for Pixy. A total of 81,462,138 records including invariant and
581 variant sites, were used to calculate π for each catch year and pairwise d_{xy} in 50kb non-
582 overlapping windows. For genome-wide nucleotide diversity for each temporal population,
583 average π value for all windows was calculated according to the equation provided by Pixy.

584 PCA on the subset of SNPs (4,685,343 after filtering for MAF > 0.01) was carried out
585 using the R package pcadapt v4.3.3 (Privé et al. 2020). Scree plots of total variance
586 explained by each principal component (PC) were examined to decide up to which PCs to
587 investigate. When all sites were included, a unique clustering pattern driven by inversion
588 status of individuals appeared (Figure S14). Thus, sites within the inverted regions (identified
589 as described in *Identifying inversion status*) were excluded then pruned based on linkage
590 disequilibrium (2,030,929 SNPs) to examine the remaining population structure.

591 Weir and Cockerham's F_{st} was calculated using vcftools v0.1.16 in 20kb windows. Only
592 weighted F_{st} was used for plotting and interpretation of the data. All plots were created in R
593 (R Development Core Team, 2022) using the base “plot” function.

594

595 **Genome-wide Temporal Covariance and Simulation**

596 Genome-wide temporal covariance was calculated using a modified python script in
597 Jupyter notebook based on the functions in cvtkpy (<http://github.com/vsbuffalo/cvtk>)
598 published in Buffalo and Coop (2020). Error bars were calculated by bootstrapping
599 covariance values, resampling blocks of loci 5000 times, using the bootstrap function
600 provided by cvtkpy. As initial genome-wide temporal covariance showed an inconclusive
601 pattern, we simulated a neutrally evolving population to compare the covariance values as a
602 control. First, backward-in-time simulation was employed to create a population with
603 matching diversity using msprime v1.2 (Baumdicker et al. 2022), with mutation rate 3.5e-9,
604 recombination rate 3.11e-8, 5000 genomes, and a sequence length of 30Mb. With this
605 population as a founding population, a forward-in-time simulation was conducted using SLiM
606 v2 (Haller and Messer 2017). Additional 100 generations were burned in at the beginning of
607 the simulated time. From generation 101, 20 individuals were sampled from the simulated
608 population for five generations, to imitate the sampling scheme of wild population. Final vcf
609 file was created to calculate the covariance of the simulated temporal populations. This was
610 replicated 100 times to create a distribution of patterns from neutrally evolving populations.

611 For the calculation of temporal covariance, a custom script in R language was used which
612 replicated the functions in cvtkpy.

613

614

615 **Genome-wide association analysis (GWA)**

616 To identify specific genomic regions responsible for growth variation in the EBC
617 population, genome-wide association study was conducted. Growth performance was
618 converted into an index using the growth estimates, $\Phi = \log k + 2 \log L^\infty$ (Moreau, Bambino,
619 and Pauly 1986; Munro and Pauly 1983). Subsequently, this variable was subjected to a
620 univariate nonlinear mixed model to identify loci associated with the growth change using
621 GEMMA v0.98.3 (Zhou and Stephens 2012). A total of 679,584 SNPs were used after
622 filtering for minor allele frequency of 0.05 and missingness of 0.1 as recommended by the
623 developers. Genetic population structure was considered as a random effect and sex as
624 covariates to incorporate and eliminate possible other contributing factors. Genomic inflation
625 factors and QQ plots showed that systematic biases were adequately corrected from the
626 other contributing factors (Figure S15). After correcting for multiple testing, using false
627 discovery rate (Benjamini and Hochberg 1995), with the number SNPs sites not in linkage
628 disequilibrium (174,541), there were no SNP sites with genome-wide significance for Wald
629 test p-values observed. Instead, as an exploratory approach to identify the loci that are most
630 likely to be associated with growth, a cutoff which includes the most obvious peaks but
631 excludes more spurious signals in the Manhattan plot were set. As results, SNP loci
632 occupying the 0.05% tail of distribution of the p-values, 338 variants, were assigned as
633 outliers for further analysis (referred to as “GWA outliers”).

634

635 **Calculating and Bootstrapping Temporal Autocovariance of GWA outliers**

636 To demonstrate the directional changes over time in allele frequencies of the GWA
637 outliers which are accountable for the growth variations, temporal covariance of the outlier
638 loci was calculated in R. We used delta values of different time windows, lag-2 and lag-3,
639 contrary to those with lag-1 provided in the cvtkpy package, which always uses consecutive
640 time points to calculate the allele frequency changes. This was to avoid including a shared
641 time point in calculating autocovariance which showed positive covariance values in the
642 simulated neutral populations and was likely driven by the shared time point rather than a
643 true signal of selection. To assess the significance of observed covariance, a permutation
644 test was conducted calculating temporal covariance values using 338 random loci sampled
645 from all SNP sites in GWA analysis. The observed values were compared to the distribution
646 of 1000 random permutations.

647

648 **Gene Identification and Gene Ontology (GO) Term Analysis**

649 To further assess the biological relevance of any outlier loci or windows from
650 genomic analysis, two approaches were employed, 1) by searching for functional
651 annotations in targeted genes for GWA outlier SNPs and 2) by gene ontology (GO) term
652 enrichment analysis using a set of outliers. For 1), among the 338 SNPs assigned as GWA
653 outliers, only regions with clustering outliers with flanking SNPs with low values (marked with
654 red arrows in Figure 12) were examined in depth. Genes located at or within 5 Kb up- and
655 downstream of the outliers were further searched for their biological functions in the
656 literature. The search was carried out using the gene names or descriptions, targeted with or
657 without key words, e.g., fish, growth, maturity, and reproduction to find the most relevant
658 functions to this study. Genes were listed by cross referencing each SNP to annotated
659 genes in the gadMor3.0 annotation database ("gmorhua_gene_ensembl") in Ensembl using
660 the BioMart v2.54.1 R package (Durinck et al. 2005). Same database and workflow were
661 used in identifying genes lying within F_{st} outlier windows and in overlapping windows of F_{st}
662 and GWA outliers. With the listed sets of genes, enriched GO terms were identified using the
663 GO terms provided in the annotations of the gadMor3.0 database as "universe." The
664 workflow was based on the vignette provided by GOstats v2.64.0 R package (Falcon and
665 Gentleman 2007).

666

667 **Identifying Inversion Status**

668 Four large (5-17 Mbp) chromosomal inversions in Atlantic cod species have been
669 previously identified (Paul R. Berg et al. 2015; Kirubakaran et al. 2016; Sodeland et al.
670 2016), three of which are polymorphic in the EBC population. We targeted these regions as
671 candidate supergenes which may have undergone selection over the study period and
672 examined how their frequency changed over time. With prior knowledge of inversions
673 located in LG2, 7 and 12, PCA was done on subset vcf files of each chromosome. Three
674 distinct clusters of individuals of different inversion status (homozygous ancestral,
675 homozygous derived, and heterozygous, "ancestral" status adopted from Matschiner et al.
676 2022) were observed, which was used for individual assignment. Then, F_{st} values were
677 calculated among these three groups (each pairwise and global) and plotted to identify
678 boundaries of the inversions (Figure S16). These boundaries were used to subset the
679 bedfiles to feed as input of local PCA analysis. The inversion status of individuals was
680 verified again by visually examining local PCA plots for each inversion status (Figure S17).
681 When ambiguous, the individuals were visually examined for their genotypes in IGV v2.12.0
682 (Thorvaldsdóttir, Robinson, and Mesirov 2013).

683 To identify the individual status of double crossover, ancestry painting was carried
684 out following a tutorial from a git repository of M. Matschiner

685 (github.com/mmatschiner/tutorials/tree/master/analysis_of_introgression_with_snp_data).
686 We used four samples (homozygotes ancestral: KIE1203003, BOR1205002 and
687 homozygotes derived: KIE1202006, KIE1203020 from Barth et al. 2019) as reference of
688 ancestral and derived homozygotes and two EBC (BOR1205003, BOR1205007; identified in
689 Matschiner et al. 2021) as “control” of double crossover. SNP sites between positions 6.5Mb
690 and 7.5Mb in LG12, (Note that the location is different than reported in Matschiner et al. as
691 different reference genomes were used) which are fixed 80% in these reference individuals,
692 allowing for 20% of missingness, were painted two different colours in EBC individuals
693 (Figure S9). Double crossover status, either ancestral/derived homozygous or heterozygous,
694 was assigned by visual examination.

695 ACKNOWLEDGEMENTS

696 **Funding:**

697 This work was funded by the Research Training Group Translational Evolutionary Research
698 (GRK 2501; project 1.1)

699

700 **Author contributions:**

701 Conceptualization: TBHR, KYH, JD
702 Sample Acquisition: KYH, TBHR, JD
703 Methodology: KYH, EEK, JD, SJ, CH, JF, BKK, KH, TBT, BDH
704 Investigation: KYH, RB, CM
705 Visualization: KYH
706 Supervision: TBHR
707 Writing—original draft: KYH, SJ, TBHR
708 Writing—review & editing: all authors

709

710 **Competing interests:**

711 Authors declare that they have no competing interests.

712

713 **Data and materials availability:**

714 The sequence data is archived under NCBI BioProject PRJNA1128530
715 The scripts and metadata used in this study are archived in a Gitlab repository
716 https://github.com/kwiyounghan/FIE_Baltic_cod

717

718 REFERENCES

719 Ahti, Pauliina A., Anna Kuparinen, and Silva Uusi-Heikkilä. 2020. "Size Does Matter — the
720 Eco-Evolutionary Effects of Changing Body Size in Fish." *Environmental Reviews* 28
721 (3): 311–24. <https://doi.org/10.1139/er-2019-0076>.

722 Anderson, Christian N. K., Chih-hao Hsieh, Stuart A. Sandin, Roger Hewitt, Anne Hollowed,
723 John Beddington, Robert M. May, and George Sugihara. 2008. "Why Fishing
724 Magnifies Fluctuations in Fish Abundance." *Nature* 452 (7189): 835–39.
725 <https://doi.org/10.1038/nature06851>.

726 Ayllon, Fernando, Erik Kjærner-Semb, Tomasz Furmanek, Vidar Wennevik, Monica F.
727 Solberg, Geir Dahle, Geir Lasse Taranger, et al. 2015. "The VgII3 Locus Controls
728 Age at Maturity in Wild and Domesticated Atlantic Salmon (*Salmo Salar L.*) Males." *PLOS Genetics* 11 (11): e1005628. <https://doi.org/10.1371/journal.pgen.1005628>.

729 Badran, Mohamed F., and Mervat A. M. Ali. 2021. "Effects of Folic Acid on Growth
730 Performance and Blood Parameters of Flathead Grey Mullet, *Mugil Cephalus*." *Aquaculture* 536 (April):736459. <https://doi.org/10.1016/j.aquaculture.2021.736459>.

731 Barghi, Neda, Joachim Hermisson, and Christian Schlötterer. 2020. "Polygenic Adaptation: A
732 Unifying Framework to Understand Positive Selection." *Nature Reviews Genetics* 21
733 (12): 769–81. <https://doi.org/10.1038/s41576-020-0250-z>.

734 Barson, Nicola J., Tutku Aykanat, Kjetil Hindar, Matthew Baranski, Geir H. Bolstad, Peder
735 Fiske, Céleste Jacq, et al. 2015. "Sex-Dependent Dominance at a Single Locus
736 Maintains Variation in Age at Maturity in Salmon." *Nature* 528 (7582): 405–8.
737 <https://doi.org/10.1038/nature16062>.

738 Barth, Julia M. I., David Villegas-Ríos, Carla Freitas, Even Moland, Bastiaan Star, Carl
739 André, Halvor Knutsen, et al. 2019. "Disentangling Structural Genomic and
740 Behavioural Barriers in a Sea of Connectivity." *Molecular Ecology* 28 (6): 1394–1411.
741 <https://doi.org/10.1111/mec.15010>.

742 Baumdicker, Franz, Gertjan Bisschop, Daniel Goldstein, Graham Gower, Aaron P Ragsdale,
743 Georgia Tsambos, Sha Zhu, et al. 2022. "Efficient Ancestry and Mutation Simulation
744 with Msprime 1.0." Edited by S Browning. *Genetics* 220 (3): iyab229.
745 <https://doi.org/10.1093/genetics/iyab229>.

746 Benjamini, Yoav, and Yosef Hochberg. 1995. "Controlling the False Discovery Rate: A
747 Practical and Powerful Approach to Multiple Testing." *Journal of the Royal Statistical
748 Society: Series B (Methodological)* 57 (1): 289–300. <https://doi.org/10.1111/j.2517-6161.1995.tb02031.x>.

749 Berg, P. R., B. Star, C. Pampoulie, I. R. Bradbury, P. Bentzen, J. A. Hutchings, S. Jentoft,
750 and K. S. Jakobsen. 2017. "Trans-Oceanic Genomic Divergence of Atlantic Cod
751 Ecotypes Is Associated with Large Inversions." *Heredity* 119 (6): 418–28.
752 <https://doi.org/10.1038/hdy.2017.54>.

753 Berg, Paul R., Sissel Jentoft, Bastiaan Star, Kristoffer H. Ring, Halvor Knutsen, Sigbjørn
754 Lien, Kjetill S. Jakobsen, and Carl André. 2015. "Adaptation to Low Salinity Promotes
755 Genomic Divergence in Atlantic Cod (*Gadus Morhua L.*)." *Genome Biology and
756 Evolution* 7 (6): 1644–63. <https://doi.org/10.1093/gbe/evv093>.

757 Bertalanffy, Ludwig von. 1957. "Quantitative Laws in Metabolism and Growth." *The Quarterly
758 Review of Biology* 32 (3): 217–31. <https://doi.org/10.1086/401873>.

759 Birgersson, Lina. 2022. "The Decline of Cod in the Baltic Sea – A Review of Biology,
760 Fisheries and Management, Including Recommendations for Cod Recovery." The
761 Fisheries Secretariat. [https://www.fishsec.org/app/uploads/2022/04/FishSec-Report-
763 Decline-Baltic-Cod-March2022.pdf](https://www.fishsec.org/app/uploads/2022/04/FishSec-Report-
762 Decline-Baltic-Cod-March2022.pdf).

764 Bosse, Mirte, Lewis G. Spurgin, Veronika N. Laine, Ella F. Cole, Josh A. Firth, Phillip
765 Gienapp, Andrew G. Gosler, et al. 2017. "Recent Natural Selection Causes Adaptive
766

768 Evolution of an Avian Polygenic Trait." *Science* 358 (6361): 365–68.
769 <https://doi.org/10.1126/science.aal3298>.

770 Brennan, Reid S, Timothy M Healy, Heather J Bryant, Man Van La, Patricia M Schulte, and
771 Andrew Whitehead. 2018. "Integrative Population and Physiological Genomics
772 Reveals Mechanisms of Adaptation in Killifish." *Molecular Biology and Evolution* 35
773 (11): 2639–53. <https://doi.org/10.1093/molbev/msy154>.

774 Buffalo, Vince, and Graham Coop. 2019. "The Linked Selection Signature of Rapid
775 Adaptation in Temporal Genomic Data." *Genetics* 213 (3): 1007–45.
776 <https://doi.org/10.1534/genetics.119.302581>.

777 ———. 2020. "Estimating the Genome-Wide Contribution of Selection to Temporal Allele
778 Frequency Change." *Proceedings of the National Academy of Sciences* 117 (34):
779 20672–80. <https://doi.org/10.1073/pnas.1919039117>.

780 Campana, Steven E. 1990. "How Reliable Are Growth Back-Calculations Based on
781 Otoliths?" *Canadian Journal of Fisheries and Aquatic Sciences* 47 (11): 2219–27.
782 <https://doi.org/10.1139/f90-246>.

783 Cardinale, M, and H Svedäng. 2011. "The Beauty of Simplicity in Science: Baltic Cod Stock
784 Improves Rapidly in a 'Cod Hostile' Ecosystem State." *Marine Ecology Progress Series*
785 Series 425 (March):297–301. <https://doi.org/10.3354/meps09098>.

786 Carstensen, Jacob, Jesper H. Andersen, Bo G. Gustafsson, and Daniel J. Conley. 2014.
787 "Deoxygenation of the Baltic Sea during the Last Century." *Proceedings of the
788 National Academy of Sciences* 111 (15): 5628–33.
789 <https://doi.org/10.1073/pnas.1323156111>.

790 Casini, Michele, Filip Käll, Martin Hansson, Maris Plikshs, Tatjana Baranova, Olle Karlsson,
791 Karl Lundström, Stefan Neuenfeldt, Anna Gårdmark, and Joakim Hjelm. 2016.
792 "Hypoxic Areas, Density-Dependence and Food Limitation Drive the Body Condition
793 of a Heavily Exploited Marine Fish Predator." *Royal Society Open Science* 3 (10):
794 160416. <https://doi.org/10.1098/rsos.160416>.

795 Cleveland, Beth M., Guangtu Gao, and Timothy D. Leeds. 2020. "Transcriptomic Response
796 to Selective Breeding for Fast Growth in Rainbow Trout (*Oncorhynchus Mykiss*)."
797 *Marine Biotechnology* 22 (4): 539–50. <https://doi.org/10.1007/s10126-020-09974-3>.

798 Cowan, Mairi, Clara Azpeleta, and Jose Fernando López-Olmeda. 2017. "Rhythms in the
799 Endocrine System of Fish: A Review." *Journal of Comparative Physiology B* 187 (8):
800 1057–89. <https://doi.org/10.1007/s00360-017-1094-5>.

801 Crespel, Amélie, Kevin Schneider, Toby Miller, Anita Rácz, Arne Jacobs, Jan Lindström,
802 Kathryn R. Elmer, and Shaun S. Killen. 2021. "Genomic Basis of Fishing-Associated
803 Selection Varies with Population Density." *Proceedings of the National Academy of
804 Sciences* 118 (51): e2020833118. <https://doi.org/10.1073/pnas.2020833118>.

805 Crespo, Diego, Jan Bogerd, Elisabeth Sambroni, Florence LeGac, Eva Andersson, Rolf B.
806 Edvardsen, Elisabeth Jönsson Bergman, Björn Thrandur Björnsson, Geir Lasse
807 Taranger, and Rüdiger W. Schulz. 2019. "The Initiation of Puberty in Atlantic Salmon
808 Brings about Large Changes in Testicular Gene Expression That Are Modulated by
809 the Energy Status." *BMC Genomics* 20 (1): 475. <https://doi.org/10.1186/s12864-019-5869-9>.

810 Czorlich, Y., T. Aykanat, J. Erkinaro, P. Orell, and C. R. Primmer. 2022. "Rapid Evolution in
811 Salmon Life History Induced by Direct and Indirect Effects of Fishing." *Science* 376
812 (6591): 420–23. <https://doi.org/10.1126/science.abg5980>.

813 Czorlich, Yann, Tutku Aykanat, Jaakko Erkinaro, Panu Orell, and Craig Robert Primmer.
814 2018. "Rapid Sex-Specific Evolution of Age at Maturity Is Shaped by Genetic
815 Architecture in Atlantic Salmon." *Nature Ecology & Evolution* 2 (11): 1800–1807.
816 <https://doi.org/10.1038/s41559-018-0681-5>.

817 Danecek, Petr, Adam Auton, Goncalo Abecasis, Cornelis A. Albers, Eric Banks, Mark A.
818 DePristo, Robert E. Handsaker, et al. 2011. "The Variant Call Format and VCFtools."
819 *Bioinformatics* 27 (15): 2156–58. <https://doi.org/10.1093/bioinformatics/btr330>.

820

821 Danecek, Petr, James K. Bonfield, Jennifer Liddle, John Marshall, Valeriu Ohan, Martin O.
822 Pollard, Andrew Whitwham, et al. 2021. "Twelve Years of SAMtools and BCFtools." *GigaScience* 10 (2): giab008. <https://doi.org/10.1093/gigascience/giab008>.

823 Davie, A., M.J.R. Porter, and N.R. Bromage. 2003. "Photoperiod Manipulation of Maturation
824 and Growth of Atlantic Cod (*Gadus Morhua*)." *Fish Physiology and Biochemistry* 28
825 (1): 399–401. <https://doi.org/10.1023/B:FISH.0000030605.19179.f8>.

826 Dobrenel, Thomas, Camila Caldana, Johannes Hanson, Christophe Robaglia, Michel
827 Vincentz, Bruce Veit, and Christian Meyer. 2016. "TOR Signaling and Nutrient
828 Sensing." *Annual Review of Plant Biology* 67 (1): 261–85.
829 <https://doi.org/10.1146/annurev-arplant-043014-114648>.

830 Durinck, Steffen, Yves Moreau, Arek Kasprzyk, Sean Davis, Bart De Moor, Alvis Brazma,
831 and Wolfgang Huber. 2005. "BioMart and Bioconductor: A Powerful Link between
832 Biological Databases and Microarray Data Analysis." *Bioinformatics* 21 (16): 3439–
833 40. <https://doi.org/10.1093/bioinformatics/bti525>.

834 Eero, Margit, Keith Brander, Tatjana Baranova, Uwe Krumme, Krzysztof Radtke, and Jane
835 W. Behrens. 2023. "New Insights into the Recent Collapse of Eastern Baltic Cod from
836 Historical Data on Stock Health." *PLOS ONE* 18 (5): e0286247.
837 <https://doi.org/10.1371/journal.pone.0286247>.

838 Eero, Margit, Joakim Hjelm, Jane Behrens, Kurt Buchmann, Massimiliano Cardinale,
839 Michele Casini, Pavel Gasyukov, et al. 2015. "Eastern Baltic Cod in Distress:
840 Biological Changes and Challenges for Stock Assessment." *ICES Journal of Marine
841 Science* 72 (8): 2180–86. <https://doi.org/10.1093/icesjms/fsv109>.

842 Eero, Margit, Brian R. MacKenzie, Friedrich W. Köster, and Henrik Gislason. 2011. "Multi-
843 Decadal Responses of a Cod (*Gadus Morhua*) Population to Human-Induced Trophic
844 Changes, Fishing, and Climate." *Ecological Applications* 21 (1): 214–26.
845 <https://doi.org/10.1890/09-1879.1>.

846 Eero, Margit, Morten Vinther, Holger Haslob, Bastian Huwer, Michele Casini, Marie Storr-
847 Paulsen, and Friedrich W. Köster. 2012. "Spatial Management of Marine Resources
848 Can Enhance the Recovery of Predators and Avoid Local Depletion of Forage Fish." *Conservation
849 Letters* 5 (6): 486–92. [https://doi.org/10.1111/j.1755-
850 263X.2012.00266.x](https://doi.org/10.1111/j.1755-263X.2012.00266.x).

851 Eikeset, Anne Maria, Andries Richter, Erin S. Dunlop, Ulf Dieckmann, and Nils Chr.
852 Stenseth. 2013. "Economic Repercussions of Fisheries-Induced Evolution." *Proceedings of the National Academy of Sciences* 110 (30): 12259–64.
853 <https://doi.org/10.1073/pnas.1212593110>.

854 Erkinaro, Jaakko, Yann Czorlich, Panu Orell, Jorma Kuusela, Morten Falkegård, Maija
855 Länsman, Henni Pulkkinen, Craig R. Primmer, and Eero Niemelä. 2019. "Life History
856 Variation across Four Decades in a Diverse Population Complex of Atlantic Salmon
857 in a Large Subarctic River." *Canadian Journal of Fisheries and Aquatic Sciences* 76
858 (1): 42–55. <https://doi.org/10.1139/cjfas-2017-0343>.

859 Falcon, S., and R. Gentleman. 2007. "Using GOstats to Test Gene Lists for GO Term
860 Association." *Bioinformatics* 23 (2): 257–58.
861 <https://doi.org/10.1093/bioinformatics/btl567>.

862 Fan, Q.C., P.F. Wu, G.J. Dai, G.X. Zhang, T. Zhang, Q. Xue, H.Q. Shi, and J.Y. Wang.
863 2017. "Identification of 19 Loci for Reproductive Traits in a Local Chinese Chicken by
864 Genome-Wide Study." *Genetics and Molecular Research* 16 (1).
865 <https://doi.org/10.4238/gmr16019431>.

866 Finn, Roderick Nigel, and Hans Jørgen Fyhn. 2010. "Requirement for Amino Acids in
867 Ontogeny of Fish." *Aquaculture Research* 41 (5): 684–716.
868 <https://doi.org/10.1111/j.1365-2109.2009.02220.x>.

869 Fonseca, Larissa Fernanda Simielli, Danielly Beraldo Dos Santos Silva, Daniele Fernanda
870 Jovino Gimenez, Fernando Baldi, Jesus Aparecido Ferro, Luis Artur Loyola
871 Chardulo, and Lucia Galvão De Albuquerque. 2020. "Gene Expression Profiling and
872 Identification of Hub Genes in Nellore Cattle with Different Marbling Score Levels." *Genomics*
873 112 (1): 873–79. <https://doi.org/10.1016/j.ygeno.2019.06.001>.

874

875

876 Franssen, S U, R. Kofler, and C. Schlötterer. 2017. "Uncovering the Genetic Signature of
877 Quantitative Trait Evolution with Replicated Time Series Data." *Heredity* 118 (1): 42–
878 51. <https://doi.org/10.1038/hdy.2016.98>.

879 Frøland Steindal, Inga A., and David Whitmore. 2019. "Circadian Clocks in Fish—What Have
880 We Learned so Far?" *Biology* 8 (1): 17. <https://doi.org/10.3390/biology8010017>.

881 Fuller, Zachary L., Veronique J. L. Mocellin, Luke A. Morris, Neal Cantin, Jianne Shepherd,
882 Luke Sarre, Julie Peng, et al. 2020. "Population Genetics of the Coral Acropora
883 Millepora: Toward Genomic Prediction of Bleaching." *Science* 369 (6501): eaba4674.
884 <https://doi.org/10.1126/science.aba4674>.

885 Fyhn, Hans Jørgen, Roderick Nigel Finn, Michael Reith, and Birgitta Norberg. 1999. "Yolk
886 Protein Hydrolysis and Oocyte Free Amino Acids as Key Features in the Adaptive
887 Evolution of Teleost Fishes to Seawater." *Sarsia* 84 (5–6): 451–56.
888 <https://doi.org/10.1080/00364827.1999.10807350>.

889 Haller, Benjamin C., and Philipp W. Messer. 2017. "SLiM 2: Flexible, Interactive Forward
890 Genetic Simulations." *Molecular Biology and Evolution* 34 (1): 230–40.
891 <https://doi.org/10.1093/molbev/msw211>.

892 Hansen, Jon Øvrum, Gerd Marit Berge, Marie Hillestad, Åshild Krogdahl, Trina F. Galloway,
893 Halvor Holm, Jørgen Holm, and Bente Ruyter. 2008. "Apparent Digestion and
894 Apparent Retention of Lipid and Fatty Acids in Atlantic Cod (*Gadus Morhua*) Fed
895 Increasing Dietary Lipid Levels." *Aquaculture* 284 (1): 159–66.
896 <https://doi.org/10.1016/j.aquaculture.2008.07.043>.

897 Hansen, Tom, Ørjan Karlsen, Geir Lasse Taranger, Gro-Ingunn Hemre, Jens Christian
898 Holm, and Olav Sigurd Kjesbu. 2001. "Growth, Gonadal Development and Spawning
899 Time of Atlantic Cod (*Gadus Morhua*) Reared under Different Photoperiods." *Aquaculture*
900 203 (1): 51–67. [https://doi.org/10.1016/S0044-8486\(01\)00610-X](https://doi.org/10.1016/S0044-8486(01)00610-X).

901 Hardy, Ronald W., and Sadasivam J. Kaushik. 2021. *Fish Nutrition*. Academic Press.

902 Heimbrand, Yvette, Karin E. Limburg, Karin Hüssy, Michele Casini, Rajlie Sjöberg, Anne-
903 Marie Palmén Bratt, Svend-Erik Levinsky, Anastasia Karpushevskaya, Krzysztof
904 Radtke, and Jill Öhlund. 2020. "Seeking the True Time: Exploring Otolith Chemistry
905 as an Age-determination Tool." *Journal of Fish Biology* 97 (2): 552–65.
906 <https://doi.org/10.1111/jfb.14422>.

907 Helmerson, Cecilia, Peggy Weist, Marine Servane Ono Brieuc, Marius F. Maurstad,
908 Franziska Maria Schade, Jan Dierking, Christoph Petereit, et al. 2023. "Evidence of
909 Hybridization between Genetically Distinct Baltic Cod Stocks during Peak Population
910 Abundance(s)." *Evolutionary Applications* 16 (7): 1359–76.
911 <https://doi.org/10.1111/eva.13575>.

912 Hemmer-Hansen, Jakob, Karin Hüssy, Henrik Baktoft, Bastian Huwer, Dorte Bekkevold,
913 Holger Haslob, Jens-Peter Herrmann, et al. 2019. "Genetic Analyses Reveal
914 Complex Dynamics within a Marine Fish Management Area." *Evolutionary
915 Applications* 12 (4): 830–44. <https://doi.org/10.1111/eva.12760>.

916 Hendry, Andrew P., Kiyoko M. Gotanda, and Erik I. Svensson. 2017. "Human Influences on
917 Evolution, and the Ecological and Societal Consequences." *Philosophical
918 Transactions of the Royal Society B: Biological Sciences* 372 (1712): 20160028.
919 <https://doi.org/10.1098/rstb.2016.0028>.

920 Hietakangas, Ville, and Stephen M. Cohen. 2009. "Regulation of Tissue Growth through
921 Nutrient Sensing." *Annual Review of Genetics* 43 (1): 389–410.
922 <https://doi.org/10.1146/annurev-genet-102108-134815>.

923 Hüssy, Karin, Margit Eero, and Krzysztof Radtke. 2018. "Faster or Slower: Has Growth of
924 Eastern Baltic Cod Changed?" *Marine Biology Research* 14 (6): 598–609.
925 <https://doi.org/10.1080/17451000.2018.1502446>.

926 Hüssy, Karin, Maria Krüger-Johnsen, Tonny Bernt Thomsen, Benjamin Dominguez Heredia,
927 Tomas Næraa, Karin E. Limburg, Yvette Heimbrand, et al. 2021. "It's Elemental, My
928 Dear Watson: Validating Seasonal Patterns in Otolith Chemical Chronologies." *Canadian
929 Journal of Fisheries and Aquatic Sciences* 78 (5): 551–66.
930 <https://doi.org/10.1139/cjfas-2020-0388>.

931 Hutchings, Jeffrey A. 2009. "ORIGINAL ARTICLE: Avoidance of Fisheries-Induced
932 Evolution: Management Implications for Catch Selectivity and Limit Reference
933 Points." *Evolutionary Applications* 2 (3): 324–34. <https://doi.org/10.1111/j.1752-4571.2009.00085.x>.

935 ICES. 2019. "Benchmark Workshop on Baltic Cod Stocks (WKBALTCOD2)." <https://doi.org/10.17895/ICES.PUB.4984>.

937 ———. 2021. "Cod (*Gadus Morhua*) in Subdivisions 24?32, Eastern Baltic Stock (Eastern
938 Baltic Sea)." <https://doi.org/10.17895/ICES.ADVICE.7745>.

939 ———. 2022. "Baltic Fisheries Assessment Working Group (WGBFAS)." Report. ICES
940 Scientific Reports. <https://doi.org/10.17895/ices.pub.19793014.v2>.

941 John, M. J., and C. L. Mahajan. 1979. "The Physiological Response of Fishes to a
942 Deficiency of Cyanocobalamin and Folic Acid." *Journal of Fish Biology* 14 (2): 127–
943 33. <https://doi.org/10.1111/j.1095-8649.1979.tb03502.x>.

944 Karlsen, Ø., G. -I. Hemre, K. Tveit, and G. Rosenlund. 2006. "Effect of Varying Levels of
945 Macro-Nutrients and Continuous Light on Growth, Energy Deposits and Maturation in
946 Farmed Atlantic Cod (*Gadus Morhua* L.)." *Aquaculture* 255 (1): 242–54.
947 <https://doi.org/10.1016/j.aquaculture.2005.12.029>.

948 Kirubakaran, Tina Graceline, Harald Grove, Matthew P. Kent, Simen R. Sandve, Matthew
949 Baranski, Torfinn Nome, Maria Cristina De Rosa, et al. 2016. "Two Adjacent
950 Inversions Maintain Genomic Differentiation between Migratory and Stationary
951 Ecotypes of Atlantic Cod." *Molecular Ecology* 25 (10): 2130–43.
952 <https://doi.org/10.1111/mec.13592>.

953 Korunes, Katharine L., and Kieran Samuk. 2021. "Pixy: Unbiased Estimation of Nucleotide
954 Diversity and Divergence in the Presence of Missing Data." *Molecular Ecology
955 Resources* 21 (4): 1359–68. <https://doi.org/10.1111/1755-0998.13326>.

956 Köster, Friedrich W., Bastian Huwer, Hans-Harald Hinrichsen, Viola Neumann, Andrei
957 Makarchouk, Margit Eero, Burkhard V. Dewitz, et al. 2017. "Eastern Baltic Cod
958 Recruitment Revisited—Dynamics and Impacting Factors." *ICES Journal of Marine
959 Science* 74 (1): 3–19. <https://doi.org/10.1093/icesjms/fsw172>.

960 Le Cren, E. D. 1951. "The Length-Weight Relationship and Seasonal Cycle in Gonad Weight
961 and Condition in the Perch (*Perca Fluviatilis*)."*Journal of Animal Ecology* 20 (2):
962 201–19. <https://doi.org/10.2307/1540>.

963 Limburg, Karin E., and Michele Casini. 2018. "Effect of Marine Hypoxia on Baltic Sea Cod
964 *Gadus Morhua*: Evidence From Otolith Chemical Proxies." *Frontiers in Marine
965 Science* 5. <https://www.frontiersin.org/articles/10.3389/fmars.2018.00482>.

966 ———. 2019. "Otolith Chemistry Indicates Recent Worsened Baltic Cod Condition Is Linked
967 to Hypoxia Exposure." *Biology Letters* 15 (12): 20190352.
968 <https://doi.org/10.1098/rsbl.2019.0352>.

969 Lin, Yu-Hung, Hui-You Lin, and Shi-Yen Shiau. 2011. "Dietary Folic Acid Requirement of
970 Grouper, *Epinephelus Malabaricus*, and Its Effects on Non-Specific Immune
971 Responses." *Aquaculture* 317 (1): 133–37.
972 <https://doi.org/10.1016/j.aquaculture.2011.04.010>.

973 Martínez-García, Lourdes, Giada Ferrari, Tom Oosting, Rachel Ballantyne, Inge van der
974 Jagt, Ingrid Ystgaard, Jennifer Harland, et al. 2021. "Historical Demographic
975 Processes Dominate Genetic Variation in Ancient Atlantic Cod Mitogenomes."
976 *Frontiers in Ecology and Evolution* 9.
977 <https://www.frontiersin.org/articles/10.3389/fevo.2021.671281>.

978 Matschiner, Michael, Julia Maria Isis Barth, Ole Kristian Tørresen, Bastiaan Star, Helle
979 Tessand Baalsrud, Marine Servane Ono Brieuc, Christophe Pampoulie, Ian
980 Bradbury, Kjetill Sigurd Jakobsen, and Sissel Jentoft. 2022. "Supergene Origin and
981 Maintenance in Atlantic Cod." *Nature Ecology & Evolution* 6 (4): 469–81.
982 <https://doi.org/10.1038/s41559-022-01661-x>.

983 Meier, H. E. Markus, Christian Dieterich, Matthias Gröger, Cyril Dutheil, Florian Börgel,
984 Kseniia Safonova, Ole B. Christensen, and Erik Kjellström. 2022. "Oceanographic

1040 Dieter Ebert and Molly Przeworski. *eLife* 11 (May):e72905.
1041 <https://doi.org/10.7554/eLife.72905>.

1042 Pauly, Daniel, and William W. L. Cheung. 2018. "Sound Physiological Knowledge and
1043 Principles in Modeling Shrinking of Fishes under Climate Change." *Global Change
1044 Biology* 24 (1): e15–26. <https://doi.org/10.1111/gcb.13831>.

1045 Pelletier, D., J. -D. Dutil, P. Blier, and H. Guderley. 1994. "Relation between Growth Rate
1046 and Metabolic Organization of White Muscle, Liver and Digestive Tract in Cod,
1047 *Gadus Morhua*." *Journal of Comparative Physiology B* 164 (3): 179–90.
1048 <https://doi.org/10.1007/BF00354078>.

1049 Pinsky, Malin L., Anne Maria Eikeset, Cecilia Helmerson, Ian R. Bradbury, Paul Bentzen,
1050 Corey Morris, Agata T. Gondek-Wyrozemska, et al. 2021. "Genomic Stability through
1051 Time despite Decades of Exploitation in Cod on Both Sides of the Atlantic." *Proceedings of the National Academy of Sciences* 118 (15): e2025453118.
1052 <https://doi.org/10.1073/pnas.2025453118>.

1053 Reid, Brendan N., Bastiaan Star, and Malin L. Pinsky. 2023. "Detecting Parallel Polygenic
1054 Adaptation to Novel Evolutionary Pressure in Wild Populations: A Case Study in
1055 Atlantic Cod (*Gadus Morhua*)." *Philosophical Transactions of the Royal Society B:
1056 Biological Sciences* 378 (1881): 20220190. <https://doi.org/10.1098/rstb.2022.0190>.

1057 Reusch, Thorsten B. H., Jan Dierking, Helen C. Andersson, Erik Bonsdorff, Jacob
1058 Carstensen, Michele Casini, Mikolaj Czajkowski, et al. 2018. "The Baltic Sea as a
1059 Time Machine for the Future Coastal Ocean." *Science Advances* 4 (5): eaar8195.
1060 <https://doi.org/10.1126/sciadv.aar8195>.

1061 Righton, Da, Kh Andersen, F Neat, V Thorsteinsson, P Steingrund, H Svedäng, K
1062 Michalsen, et al. 2010. "Thermal Niche of Atlantic Cod *Gadus Morhua*: Limits,
1063 Tolerance and Optima." *Marine Ecology Progress Series* 420 (December):1–13.
1064 <https://doi.org/10.3354/meps08889>.

1065 Roff, Derek. 1993. *Evolution Of Life Histories: Theory and Analysis*. Springer Science &
1066 Business Media.

1067 Sánchez-Vázquez, Francisco Javier, Jose Fernando López-Olmeda, Luisa Maria Vera,
1068 Herve Migaud, Marcos Antonio López-Patiño, and Jesús M. Míguez. 2019.
1069 "Environmental Cycles, Melatonin, and Circadian Control of Stress Response in
1070 Fish." *Frontiers in Endocrinology* 10.
1071 <https://www.frontiersin.org/articles/10.3389/fendo.2019.00279>.

1072 Sardell, Jason M., and Mark Kirkpatrick. 2020. "Sex Differences in the Recombination
1073 Landscape." *The American Naturalist* 195 (2): 361–79.
1074 <https://doi.org/10.1086/704943>.

1075 Schenk, Hanna, Fabian Zimmermann, and Martin Quaas. 2023. "The Economics of
1076 Reversing Fisheries-Induced Evolution." *Nature Sustainability* 6 (6): 706–11.
1077 <https://doi.org/10.1038/s41893-023-01078-9>.

1078 Schmölcke, Ulrich, Elisabeth Endtmann, Stefanie Klooss, Michael Meyer, Dierk Michaelis,
1079 Björn-Henning Rickert, and Doreen Rößler. 2006. "Changes of Sea Level,
1080 Landscape and Culture: A Review of the South-Western Baltic Area between 8800
1081 and 4000BC." *Palaeogeography, Palaeoclimatology, Palaeoecology* 240 (3): 423–38.
1082 <https://doi.org/10.1016/j.palaeo.2006.02.009>.

1083 Siegel, Herbert, and Monika Gerth. 2018 "Sea Surface Temperature in the Baltic Sea 2018."
1084 Skulstad, Ole Fredrik, John Taylor, Andrew Davie, Herve Migaud, Tore Kristiansen, Ian
1085 Mayer, Geir Lasse Taranger, Rolf Erik Olsen, and Ørjan Karlsen. 2013. "Effects of
1086 Light Regime on Diurnal Plasma Melatonin Levels and Vertical Distribution in Farmed
1087 Atlantic Cod (*Gadus Morhua* L.)." *Aquaculture* 414–415 (November):280–87.
1088 <https://doi.org/10.1016/j.aquaculture.2013.08.007>.

1089 Sodeland, Marte, Per Erik Jorde, Sigmund Lien, Sissel Jentoft, Paul R. Berg, Harald Grove,
1090 Matthew P. Kent, Mariann Arnyasi, Esben Moland Olsen, and Halvor Knutsen. 2016.
1091 "Islands of Divergence' in the Atlantic Cod Genome Represent Polymorphic
1092 Chromosomal Rearrangements." *Genome Biology and Evolution* 8 (4): 1012–22.
1093 <https://doi.org/10.1093/gbe/evw057>.

1094

1095 Stockmayer, Vera, and Andreas Lehmann. 2023. "Variations of Temperature, Salinity and
1096 Oxygen of the Baltic Sea for the Period 1950 to 2020." *Oceanologia* 65 (3): 466–83.
1097 <https://doi.org/10.1016/j.oceano.2023.02.002>.

1098 Stubhaug, I., Ø. Lie, and B.e. Torstensen. 2007. "Fatty Acid Productive Value and β -
1099 Oxidation Capacity in Atlantic Salmon (*Salmo Salar L.*) Fed on Different Lipid
1100 Sources along the Whole Growth Period." *Aquaculture Nutrition* 13 (2): 145–55.
1101 <https://doi.org/10.1111/j.1365-2095.2007.00462.x>.

1102 Su, Yu-Sung, and Masanao Yajima. 2021. "R2jags: Using R to Run 'JAGS.'" R.
1103 <https://CRAN.R-project.org/package=R2jags>.

1104 Svedäng, Henrik, and Sara Hornborg. 2014. "Selective Fishing Induces Density-Dependent
1105 Growth." *Nature Communications* 5 (1): 4152. <https://doi.org/10.1038/ncomms5152>.

1106 ———. 2017. "Historic Changes in Length Distributions of Three Baltic Cod (*Gadus Morhua*
1107) Stocks: Evidence of Growth Retardation." *Ecology and Evolution* 7 (16): 6089–
1108 6102. <https://doi.org/10.1002/ece3.3173>.

1109 Takahashi, Takayuki, and Katsueki Ogiwara. 2023. "cAMP Signaling in Ovarian Physiology
1110 in Teleosts: A Review." *Cellular Signalling* 101 (January):110499.
1111 <https://doi.org/10.1016/j.cellsig.2022.110499>.

1112 Taranger, Geir Lasse, Manuel Carrillo, Rüdiger W. Schulz, Pascal Fontaine, Silvia Zanuy,
1113 Alicia Felip, Finn-Arne Weltzien, et al. 2010. "Control of Puberty in Farmed Fish."
1114 *General and Comparative Endocrinology, Fish Reproduction*, 165 (3): 483–515.
1115 <https://doi.org/10.1016/j.ygcen.2009.05.004>.

1116 Thorvaldsdóttir, Helga, James T. Robinson, and Jill P. Mesirov. 2013. "Integrative Genomics
1117 Viewer (IGV): High-Performance Genomics Data Visualization and Exploration."
1118 *Briefings in Bioinformatics* 14 (2): 178–92. <https://doi.org/10.1093/bib/bbs017>.

1119 Tigano, Anna, Arne Jacobs, Aryn P Wilder, Ankita Nand, Ye Zhan, Job Dekker, and Nina
1120 Overgaard Therkildsen. 2021. "Chromosome-Level Assembly of the Atlantic
1121 Silverside Genome Reveals Extreme Levels of Sequence Diversity and Structural
1122 Genetic Variation." *Genome Biology and Evolution* 13 (6): evab098.
1123 <https://doi.org/10.1093/gbe/evab098>.

1124 Trichet, Viviane Verlhac. 2010. "Nutrition and Immunity: An Update." *Aquaculture Research*
1125 41 (3): 356–72. <https://doi.org/10.1111/j.1365-2109.2009.02374.x>.

1126 Turchini, Giovanni M., and David S. Francis. 2009. "Fatty Acid Metabolism (Desaturation,
1127 Elongation and β -Oxidation) in Rainbow Trout Fed Fish Oil- or Linseed Oil-Based
1128 Diets." *British Journal of Nutrition* 102 (1): 69–81.
1129 <https://doi.org/10.1017/S0007114508137874>.

1130 Vitousek, Peter M., Harold A. Mooney, Jane Lubchenco, and Jerry M. Melillo. 1997. "Human
1131 Domination of Earth's Ecosystems." *Science* 277 (5325): 494–99.
1132 <https://doi.org/10.1126/science.277.5325.494>.

1133 Zeller, D., P. Rossing, S. Harper, L. Persson, S. Booth, and D. Pauly. 2011. "The Baltic Sea:
1134 Estimates of Total Fisheries Removals 1950–2007." *Fisheries Research* 108 (2):
1135 356–63. <https://doi.org/10.1016/j.fishres.2010.10.024>.

1136 Zhdanova, Irina, and Stéphan Reebs. 2006. "Circadian Rhythms in Fish." In *Fish Physiology*,
1137 24:197–238. [https://doi.org/10.1016/S1546-5098\(05\)24006-2](https://doi.org/10.1016/S1546-5098(05)24006-2).

1138 Zhou, Xiang, and Matthew Stephens. 2012. "Genome-Wide Efficient Mixed-Model Analysis
1139 for Association Studies." *Nature Genetics* 44 (7): 821–24.
1140 <https://doi.org/10.1038/ng.2310>.

1141 Zillén, Lovisa, Daniel J. Conley, Thomas Andrén, Elinor Andrén, and Svante Björck. 2008.
1142 "Past Occurrences of Hypoxia in the Baltic Sea and the Role of Climate Variability,
1143 Environmental Change and Human Impact." *Earth-Science Reviews* 91 (1): 77–92.
1144 <https://doi.org/10.1016/j.earscirev.2008.10.001>.

1145

1146

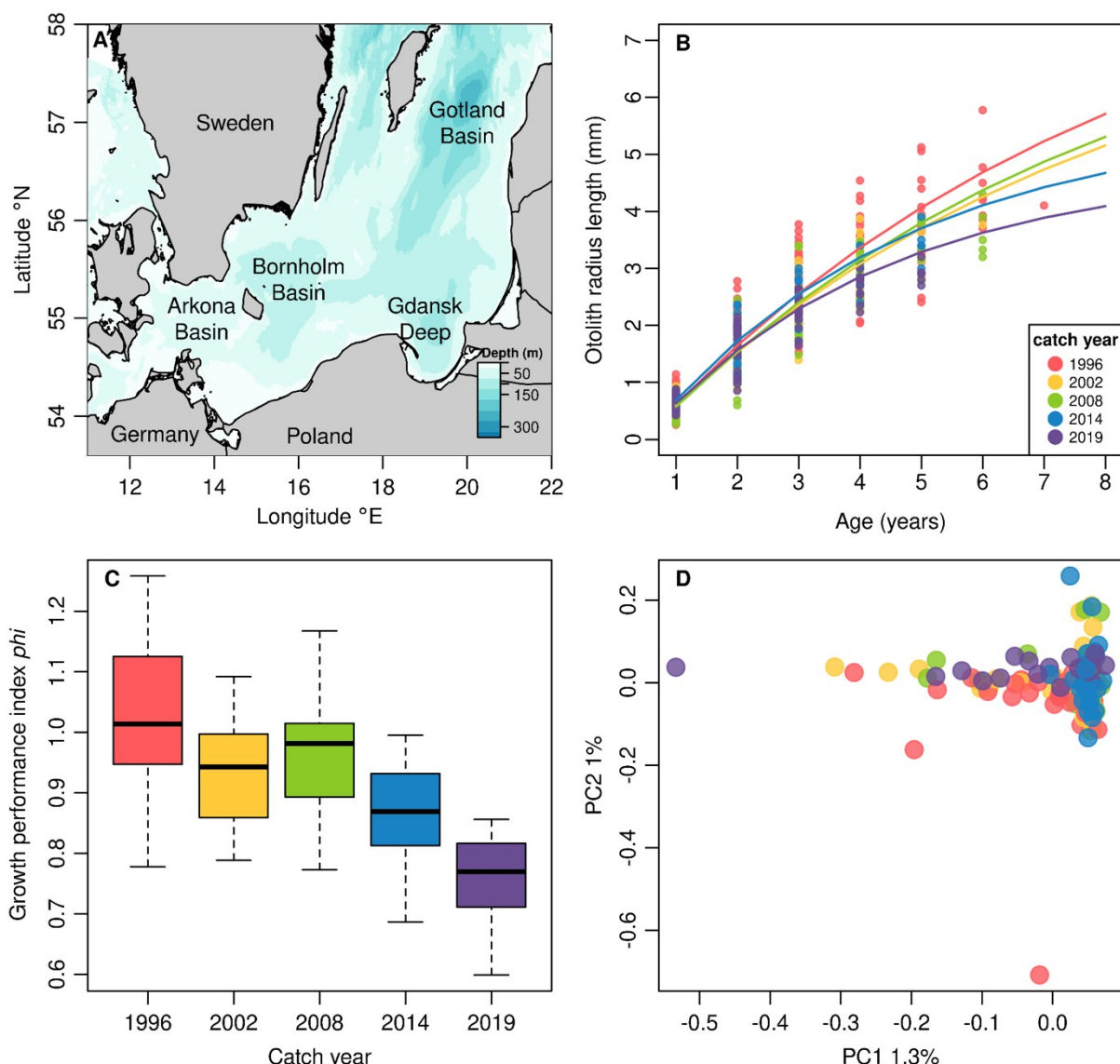
1147

1148

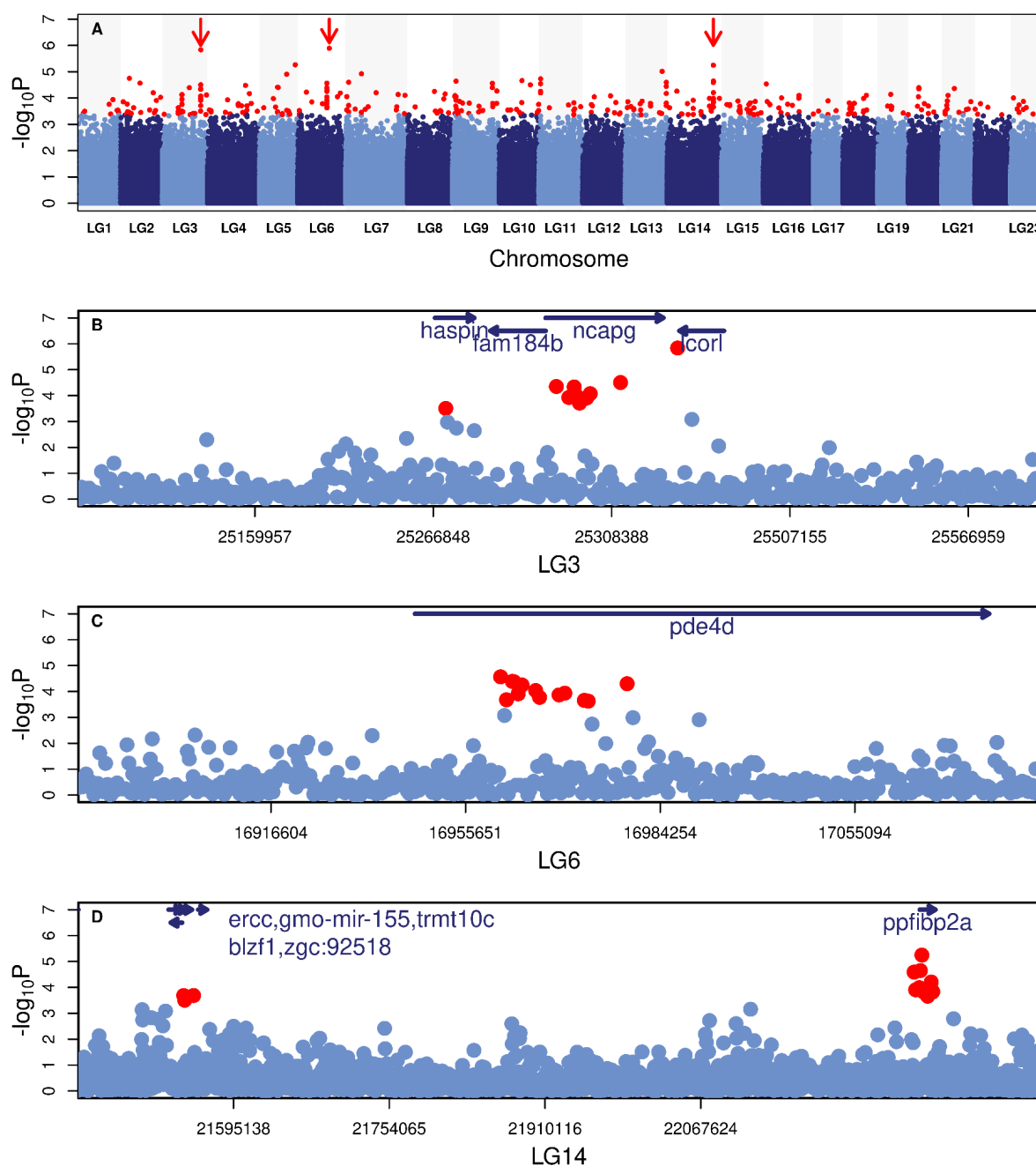
1149

1150 **Figure 1. Sampling location in the Baltic Sea and population response over time**

1151 **A.** Map of the Baltic Sea showing the sampling sites in Bornholm Basin, the major spawning
1152 ground for EBC. Their spawning grounds in Gotland Basin and Gdansk Deep are not
1153 recognized as viable anymore. **B.** Estimated von Bertalanffy growth curves for each catch
1154 year. The von Bertalanffy growth curves are based on otolith readings and were plotted
1155 using estimated sets of parameters for each temporal population of "random" and
1156 "phenotype" samples. The temporal group 1996 in this figure also includes "phenotype"
1157 samples (catch year from 1996-1998) as they are treated as one temporal population in the
1158 model. Each point depicts observed otolith radius to chemical annuli at age coloured based
1159 on the individuals' catch year. **C.** Boxplots of individual growth performance, Φ , calculated
1160 using estimated individual von Bertalanffy growth parameters (L^∞ and k) over time. Colour
1161 codes are based on individuals' catch years as in the legend in panel B. **D.** Principal
1162 component analysis of 115 "random" samples. A set of SNPs were pruned based on linkage
1163 disequilibrium and removed of sites within the inversions in LG2, 7, and 12. PC1 explains
1164 1.3%, and 1% for PC2, of all variations in the genotypes. Each individual is coded in colour
1165 according to the catch years as in legend in panel B.

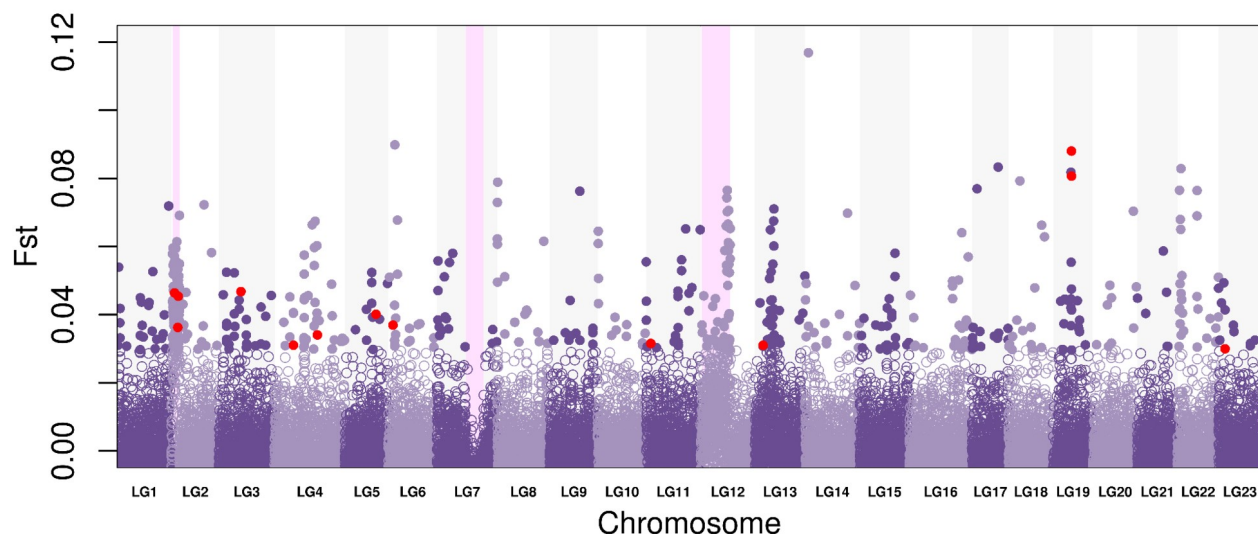


1166 **Figure 2. Manhattan plot of -logP values in genome-wide association (GWA) analysis.**
1167 **A.** Manhattan plot of -logP values in genome-wide association (GWA) analysis. A total of
1168 152 samples were subjected to GWA using the sequenced genotypes, 679,584 SNPs (>0.05
1169 MAF), and estimated growth performance index Φ as phenotype. Negative log transformed
1170 Wald test p-values for each SNP were plotted along the genome. Outlier status was
1171 assigned for 338 SNPs with lowest 0.05% p-values (in red circles). The cutoff for outliers
1172 were selected based on the visual examination of this Manhattan plot, so as to include
1173 distinctive peaks with clustering outliers (marked with red arrows) and at the same time
1174 exclude spurious outliers consisting of single SNPs only. Regions marked with red arrows
1175 were zoomed in, **B.** in LG3 **C.** LG6, and **D.** LG14 and genes residing at or near (5 Kb up-
1176 and downstream) the outliers are annotated (Table 1).



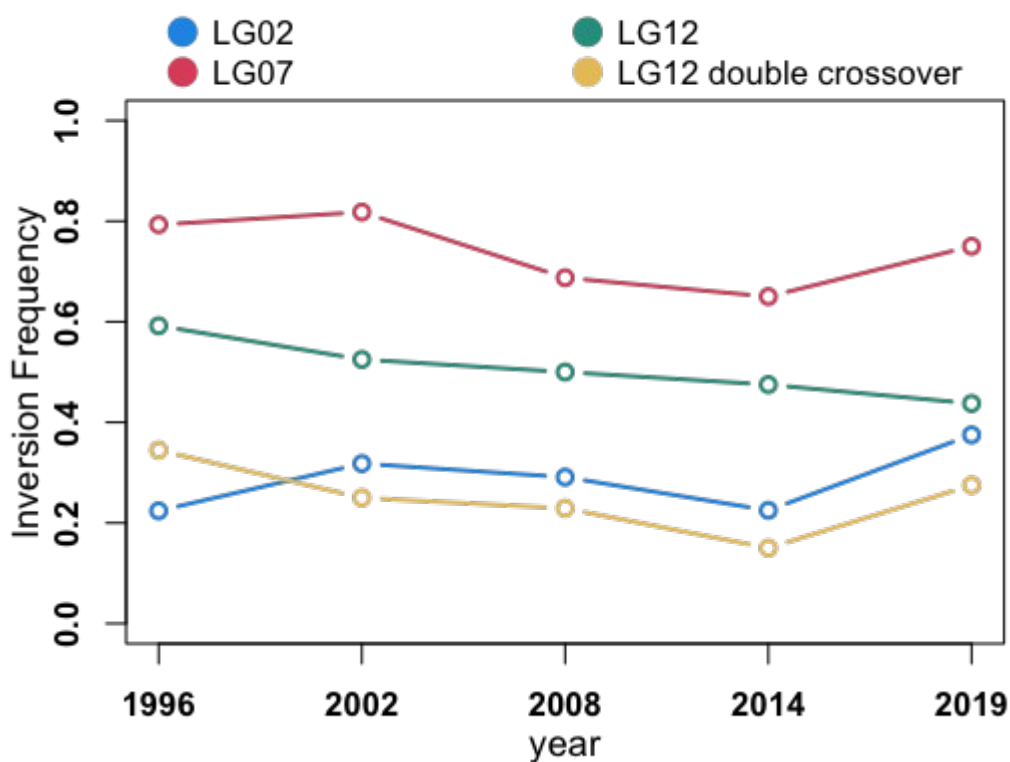
1177 **Figure 3. F_{st} values in 20kb windows along the genome.**

1178 Pairwise F_{st} values of 1996 and 2019 in 20 Kb non-overlapping windows were calculated
1179 along the whole genome. Filled purple points indicate the highest top 5% of genome-wide F_{st}
1180 outlier windows. Regions with exceptionally high and low F_{st} values show the inverted
1181 regions in cod genome in LG2, LG7, and LG12 and were marked with pink shades. Among
1182 outlier windows, windows overlapping with GWA outliers were marked as red.



1183 **Figure 4. Frequency change of inversion haplotypes.**

1184 The frequency of ancestral allele of each inverted region in LG2, LG7, and LG12, and the
1185 double crossover within LG12 are plotted over study period. The inversions in LG2 and LG7
1186 display an inconsistent pattern. For the inversion in LG12, a monotonic decrease in
1187 frequency over time is observed that is statistically significant (Mann-Kendall test for
1188 monotonic trend: p-value = 0.03), whereas the frequency of double crossover within the
1189 region changes independently.



1191 **Table 1. A list of genes intersecting or neighbouring with GWA outlier SNPs with its
1192 position and description.**

1193 A list of genes unique in the "ensembl_gene_id" located at or 10 Kb surrounding regions of
1194 GWA outlier SNPs was subjected to a search for their functional annotations in the literature.
1195 Columns, ensembl_gene_id, chromosome_name, external_gene_name, description,
1196 start_position, and end_position, are annotations in the gadMor3.0 reference genome
1197 extracted from Ensembl database. When the external_gene_name were not provided by the
1198 database, search in the NCBI gene database or orthologs' name were filled in (Genes,
1199 NCBI). Functional annotations of the genes, in the most relevant context to this study,
1200 "known biological functions from literature", were listed by searching the gene names with or
1201 without keywords (e.g., fish, growth, weight, maturity, and reproduction) in the literature
1202 search. When there were no search results which showed direct or indirect biological
1203 relevance in the targeted context, they were marked as "Not found in literature". Some
1204 genes were catalogued with only weak matches to orthologs in other species in the
1205 database, thus marked as "NA (Not applicable)". Rows containing genes which are most
1206 relevant to this study are highlighted in grey.

ensembl_gene_id	external_gene_name	chromosome_name	known biological functions from literature	description	start_position	end_position
At the outlier loci						
ENSGMOG00000032747	HEPACAM	3	cell-adhesion, cell motility, cancer suppressor gene	carcinoembryonic antigen-related cell adhesion molecule 6-like [Source:NCBI gene (formerly Entrezgene);Acc:115540996]	13790699	13856484
ENSGMOG00000015953	mnd1	3	meiotic arrest, recombination	meiotic nuclear divisions 1 homolog (S. cerevisiae) [Source:NCBI gene (formerly Entrezgene);Acc:115540214]	20677607	20683019
ENSGMOG00000012895	NA	3	NA	NA	21756782	21778636
ENSGMOG00000016255	haspin	3	mitosis, critical larval growth and survival in zebrafish	histone H3 associated protein kinase [Source:NCBI gene (formerly Entrezgene);Acc:115540151]	25267491	25278374
ENSGMOG00000016202	ncapg	3	DEGs in salmon puberty	non-SMC condensin I complex, subunit G [Source:NCBI gene (formerly Entrezgene);Acc:115540152]	25305001	25318049
ENSGMOG00000007843	PDE4D	6	a rainbow trout line selectively bred for fast growth (growth line, GL) . Transcriptomic response . Several key components of the cAMP signaling pathway were reduced in the GL, including adenylate cyclase-type 6 (adcy6) and phosphodiesterase 4D (pde4d)	phosphodiesterase 4D, cAMP-specific [Source:NCBI gene (formerly Entrezgene);Acc:115545011]	16947270	17078303
ENSGMOG00000013441	trpm1b	9	retina pigment development	transient receptor potential cation channel subfamily M member 1-like [Source:NCBI gene (formerly	21730570	21750419

				Entrezgene);Acc:115550405]		
ENSGMOG00000037198	ciart	9	Transcriptional changes in the process of reproductive hormone affecting circadian rythm in zebrafish. generally circadian regulation of gene expression	circadian-associated transcriptional repressor-like [Source:NCBI gene (formerly Entrezgene);Acc:115550867]	21823470	21831852
ENSGMOG00000017135	coro1ca	13	Not found in literature	coronin, actin binding protein, 1Ca [Source:NCBI gene (formerly Entrezgene);Acc:115556521]	25841273	25924738
ENSGMOG00000008588	ercc5	14	higher rate of malformations and decreased embryo viability in fish, COFS syndrome in human.	excision repair cross-complementation group 5 [Source:NCBI gene (formerly Entrezgene);Acc:115558732]	21543979	21552546
ENSGMOG00000016695	PPFIBP2 (orthologs)	14	human fetal abnormality	PPFIA binding protein 2a [Source:ZFIN;Acc:ZDB-GENE-070705-277]	22269074	22285193
ENSGMOG00000018629	kcnk2b (ortholog)	21	increased expression during puberty in zebrafish	NA	4143319	4168663
ENSGMOG00000013114	snx17	21	intracellular protein transport, in a conserved genomic region (together with atraid) associated with miR-133b which is involved in oogenesis in a tilapia	sorting nexin 17 [Source:NCBI gene (formerly Entrezgene);Acc:115534617]	4307230	4333109

5 Kb up- and down-stream

ENSGMOG00000026566	NA	3	NA	NA	13810816	13811780
ENSGMOG00000015878	TMEM131L	3	Not found in literature	transmembrane 131 like [Source:NCBI gene (formerly Entrezgene);Acc:115540213]	20642815	20676221
ENSGMOG00000030622	NA	3	NA	NA	25275974	25276992
ENSGMOG00000036363	fam184b	3	chicken body weight at first egg	family with sequence similarity 184 member B [Source:NCBI gene (formerly Entrezgene);Acc:115540150]	25280244	25303554
ENSGMOG00000022331	lcrl	3	human: Expression of the LCRL gene was significantly associated with length of the neonate at birth	ligand dependent nuclear receptor corepressor-like [Source:NCBI gene (formerly Entrezgene);Acc:115540149]	25319776	25337592
ENSGMOG00000036563	NA	13	NA	NA	25928210	25928944
ENSGMOG00000033950	cenpq	14	Not found in literature	centromere protein Q [Source:NCBI gene (formerly Entrezgene);Acc:115559135]	21398766	21402387
ENSGMOG00000025157	gmo-mir-155	14	Not found in literature	gmo-mir-155 [Source:miRBase;Acc:MI0036008]	21410103	21410161
ENSGMOG00000003226	ephrin-B2a-like	14	angiogenesis	ephrin-B2a-like [Source:NCBI gene (formerly Entrezgene);Acc:115559324]	21411256	21419004
ENSGMOG00000025102	trmt10c	14	Not found in literature	tRNA methyltransferase 10C, mitochondrial RNase P subunit [Source:ZFIN;Acc:ZDB-GENE-041114-12]	21536364	21543958
ENSGMOG00000035263	blzf1	14	heart function, development in medaka	basic leucine zipper nuclear factor 1 [Source:NCBI gene (formerly Entrezgene);Acc:115558734]	21538764	21543958
ENSGMOG00000030760	mettl21e	14	linked to growth in pupfishes, intramuscular	methyltransferase like 21e [Source:NCBI gene (formerly	21552352	21557877

			fat deposition in cattle	Entrezgene);Acc:115558735]		
ENSGMOG00000024865	NA	14	differentially expressed in response to temperature in stickleback, also generally skeletal muscle development related	protein-lysine methyltransferase METTL21C-like [Source:NCBI gene (formerly Entrezgene);Acc:115558577]	21560583	21565349
ENSGMOG00000013100	atraig	21	bone differentiation	all-trans retinoic acid-induced differentiation factor [Source:NCBI gene (formerly Entrezgene);Acc:115534618]	4334479	4337000

1207

1208 **Table 2. A list of enriched GO terms using genes within Fst windows that overlap with**
1209 **GWA outlier SNPs.**

1210 To identify loci which are highly correlated with growth performance and selected over time,
1211 the intersections of Fst outlier windows and GWA outlier SNPs were investigated. When a
1212 GWA outlier SNP resides within an Fst outlier window, this window was counted as an
1213 overlapping outlier window (marked as red in Figure3). Any genes residing within these
1214 overlapping outlier windows were subjected to gene ontology (GO) enrichment test to
1215 identify any biological functions that correlate to growth performance and at the same time
1216 differentiated the most over time. P values are adjusted using false discovery rate. Only
1217 biological processes were presented among GO categories for the analysis.

GO.term	GO.name	p.value.adjusted
GO:0007624	ultradian rhythm	0.01203089399
GO:0050891	multicellular organismal water homeostasis	0.01442325268
GO:0034080	CENP-A containing chromatin assembly	0.01442325268
GO:0006546	glycine catabolic process	0.02048356121
GO:0035825	homologous recombination	0.02098495744
GO:0007131	reciprocal meiotic recombination	0.02098495744
GO:0009396	folic acid-containing compound biosynthetic process	0.02214772591
GO:0009408	response to heat	0.02678127453
GO:0000122	negative regulation of transcription by RNA polymerase II	0.0330299368
GO:0009069	serine family amino acid metabolic process	0.03431805692
GO:0140013	meiotic nuclear division	0.03509647983
GO:1901606	alpha-amino acid catabolic process	0.03509647983
GO:0042558	pteridine-containing compound metabolic process	0.03509647983
GO:0061982	meiosis I cell cycle process	0.03509647983
GO:0051321	meiotic cell cycle	0.04643225312
GO:0001755	neural crest cell migration	0.04698068426

1218